



# *Lines in the CMB spectrum from the epoch of Cosmological Recombination*

José Alberto Rubiño-Martín  
(IAC)

( In collaboration with : R.A. Sunyaev, C.Hernández-Monteagudo, J. Chluba )

Time since the Big Bang (years)

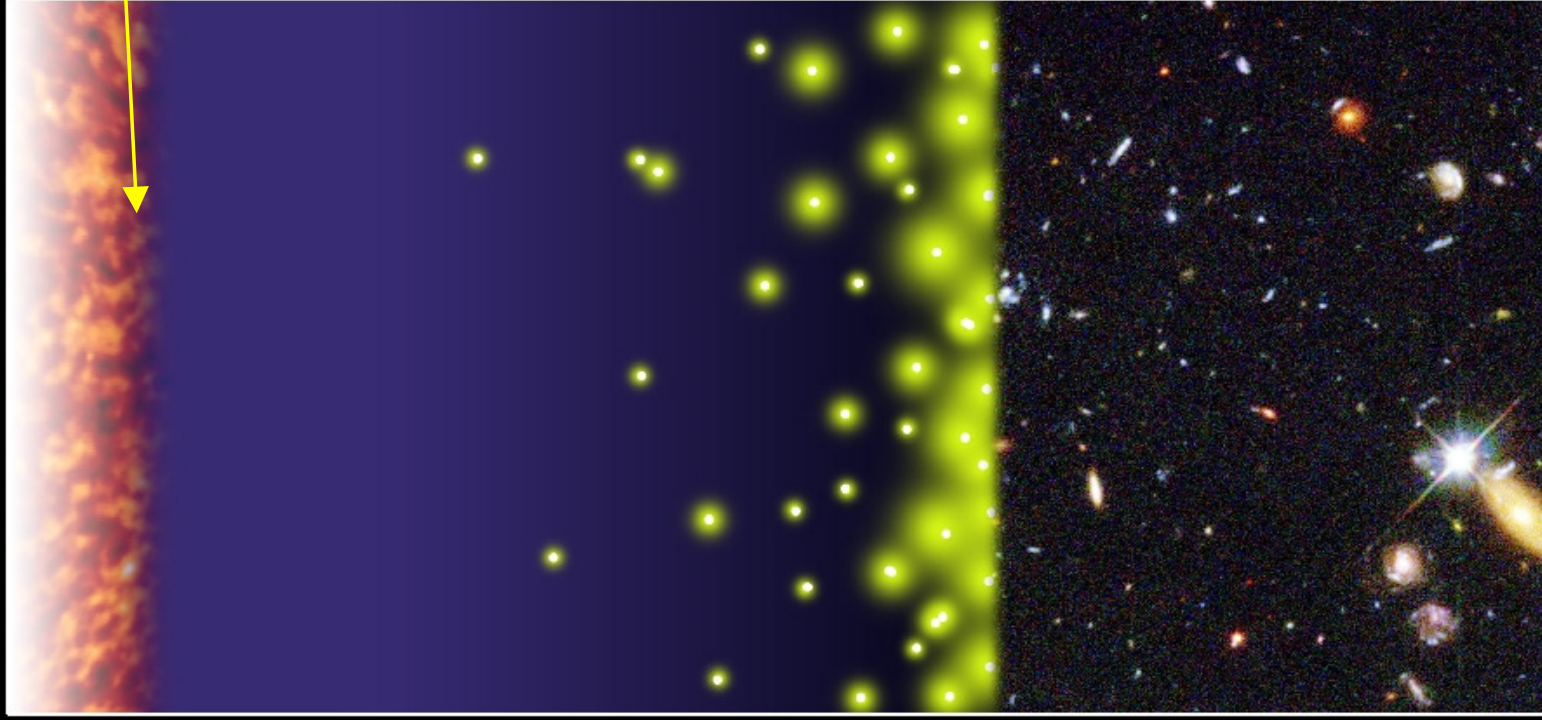
~ 300 thousand

~ 500 million

~ 1 billion

~ 9 billion

~ 13 billion



← The Big Bang

The Universe filled with ionized gas

← The Universe becomes neutral and opaque

The Dark Ages start

Galaxies and Quasars begin to form  
The Reionization starts

Pop III stars.

The Cosmic Renaissance  
The Dark Ages end

← Reionization complete, the Universe becomes transparent again

Galaxies evolve

The Solar System forms

Today: Astronomers figure it all out!

**Recombination ( $z \sim 1000$ )**  
(Microwave background)

**Dark Ages**

(Neutral hydrogen.  
Accessible with 21cm line  
surveys as SKA or LOFAR)

**$z \sim 6$**

(GP trough observed in QSO)

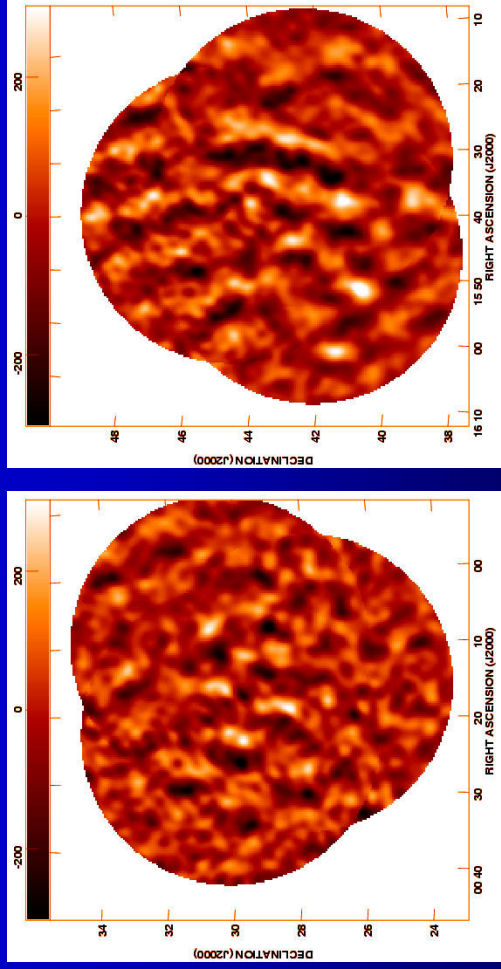
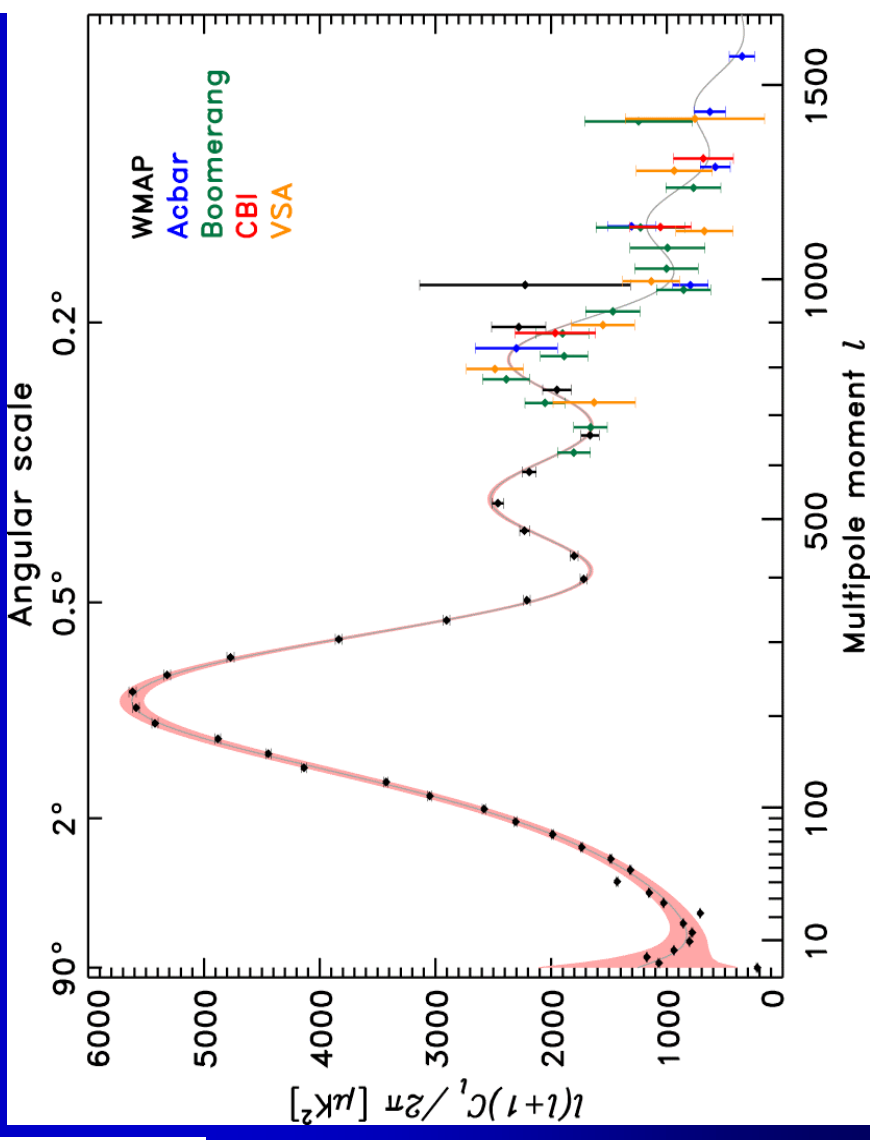
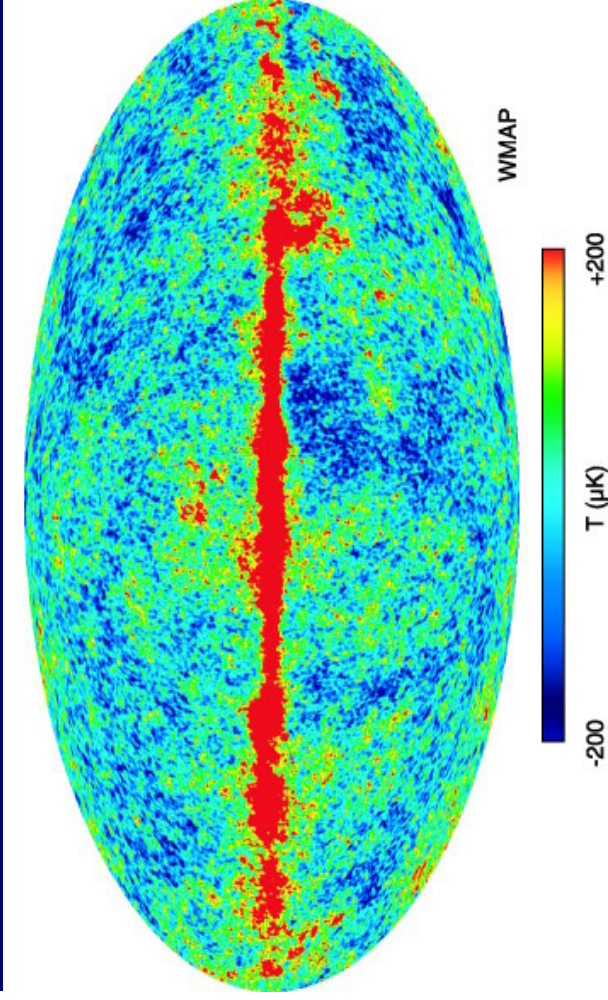
**Galaxies form and evolve**

(Universe accessible with optical/IR telescopes)

# Angular fluctuations of the CMB

## CMB anisotropies: Dynamics

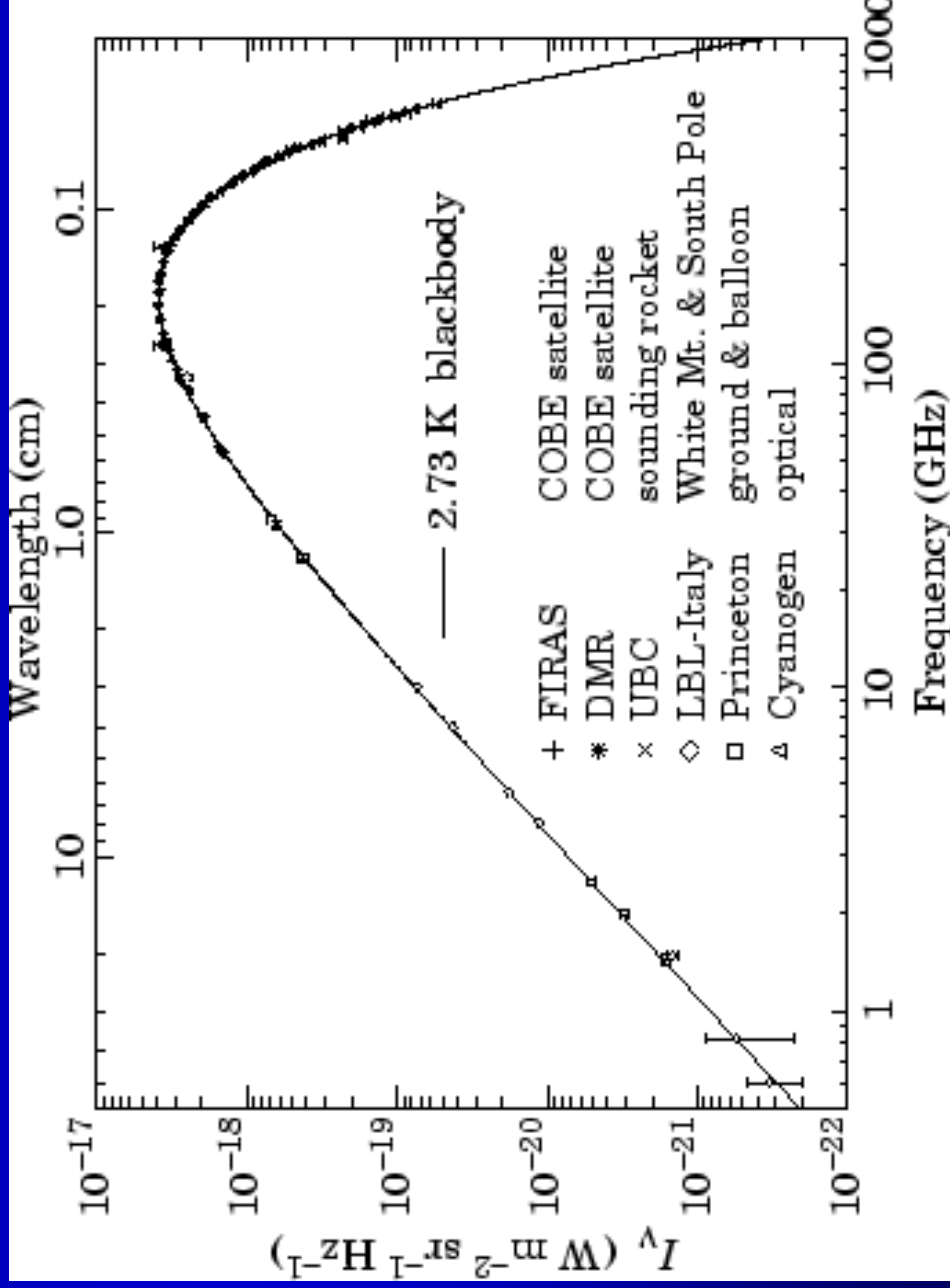
- Initial conditions (inflation)
- Cosmological parameters



VSA

# The CMB Spectrum

- Encodes information about **energetics** in the Universe (phase transitions in early universe; relic decay DM particles; reionization).



Blackbody spectrum with extremely high precision  
(FIRAS, Fixsen & Mather 2002)

$$T_0 = 2.725 \pm 0.001 \text{ K}$$
$$|\mu| < 9 \times 10^{-5} \text{ (95\% CL)}$$
$$|y| < 15 \times 10^{-6} \text{ (95\% CL)}$$

Time since the Big Bang (years)

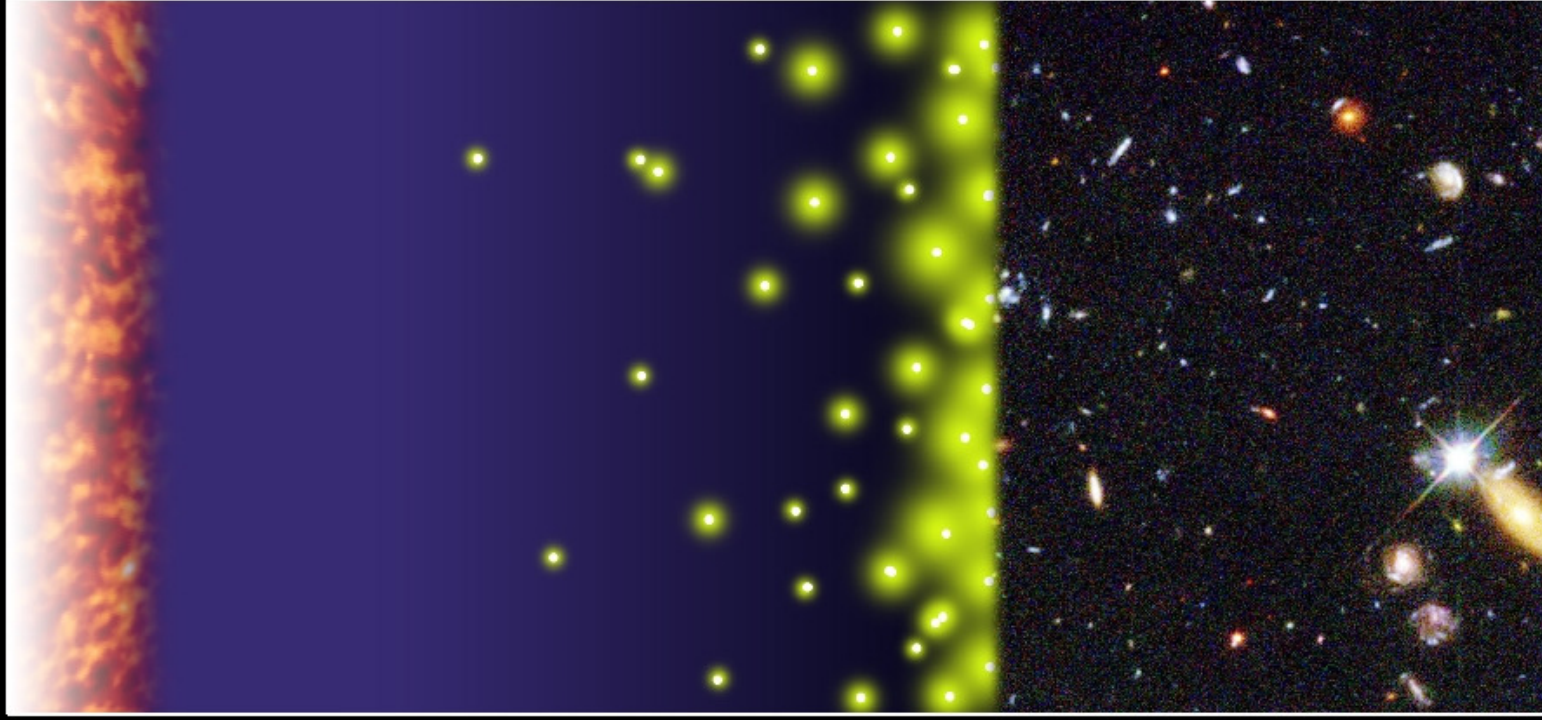
~ 300 thousand

~ 500 million

~ 1 billion

~ 9 billion

~ 13 billion



### ← The Big Bang

- The Universe filled with ionized gas
- ← The Universe becomes neutral and opaque
- The Dark Ages start

Galaxies and Quasars begin to form  
The Reionization starts

### PopIII stars?

The Cosmic Renaissance  
The Dark Ages end

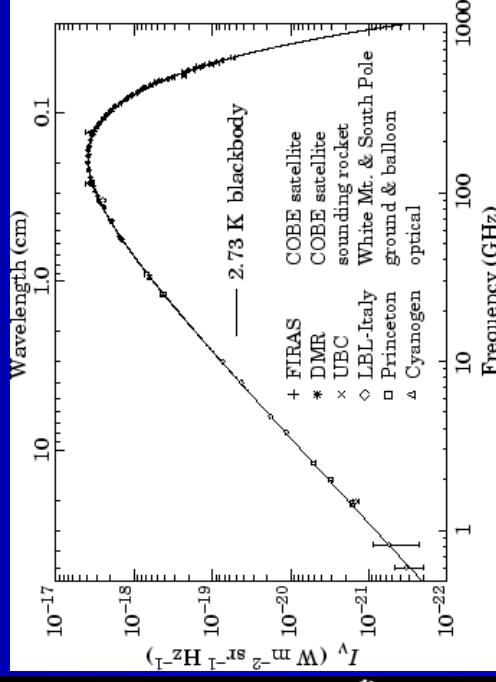
- ← Reionization complete, the Universe becomes transparent again

Galaxies evolve

The Solar System forms

Today: Astronomers figure it all out!

Is it possible to obtain spectral information from the epoch of recombination?



Or, in other words:

Where are the Ly- $\alpha$  photons from the epoch of recombination?

# *Overview*

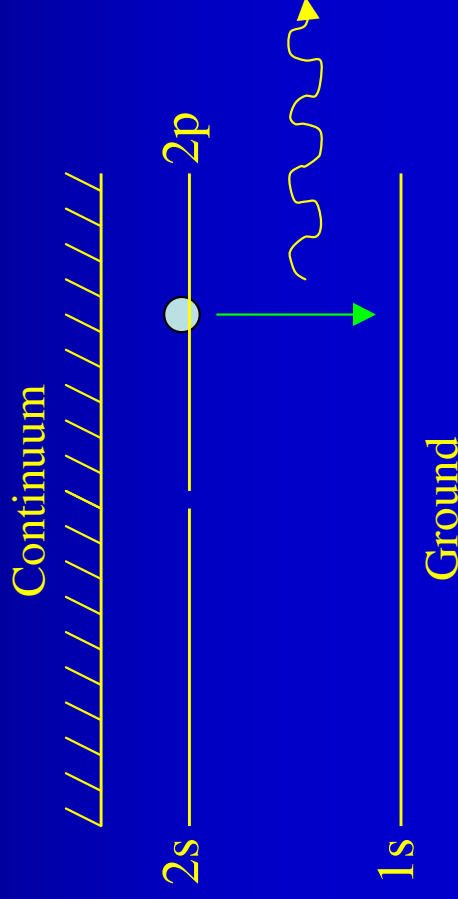
- Introduction. The Cosmological Hydrogen Recombination.
- Observing spectral features from recombination.
  - Hydrogen Spectrum from Recombination.
  - Effect on the angular power spectrum.
- Observability of the lines.
- Conclusions

# How did the Universe become neutral?

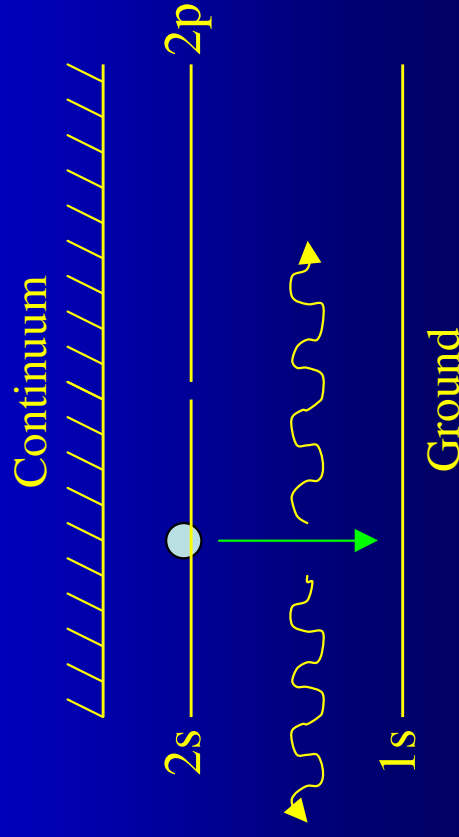
- Zel'dovich, Kurt & Sunyaev (1968) and Peebles (1968) were the first describing how the recombination occurs in the Universe.
- Two main arguments to understand Recombination:
  - Due to the high entropy of the Universe ( $\sim 1.6 \times 10^9$  photons per baryon) recombination occurs at  $z = 1000$ . (Note that  $13.6 \text{ eV} = 157800 \text{ K}$ , but  $3000 \text{ K} = 0.26 \text{ eV}$ ). In addition, collisional processes are not important.
  - The Lyman-alpha photons are optically thick (Case B recombination). The main channel of the recombination is the  $2s$  two-photon decay.

# How did the Universe become neutral? (II)

## a) Ly- $\alpha$ photon is absorbed by other atom



## b) Two photons can escape.



- Effective 3-level atom.
- Direct recombinations to ground state do not produce a net recombination.
- Ly- $\alpha$  photons are optically thick and can not redshift before being re-absorbed. Level 2 overpopulated.
- Two photon 2s decay is the main channel, but the Einstein A-coefficient is  $A_{2s1s} = 8.22 \text{ s}^{-1}$ .

**RECOMBINATION IS DELAYED**

# Where are the Ly- $\alpha$ photons from the epoch of recombination?

In the Wien tail of the Blackbody spectrum.

No. 1, 1968

PRIMEVAL PLASMA

9

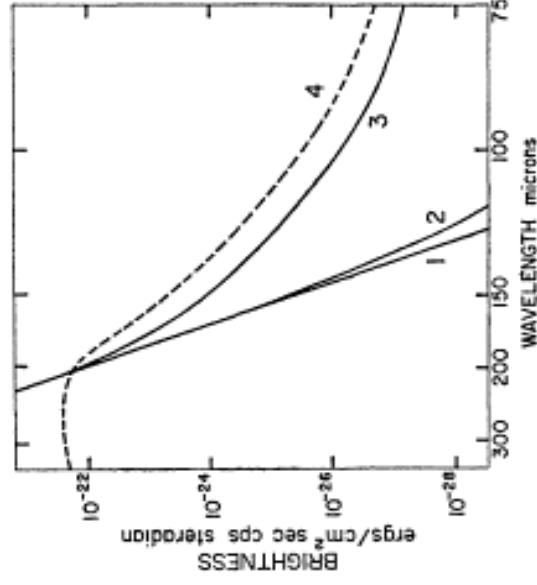
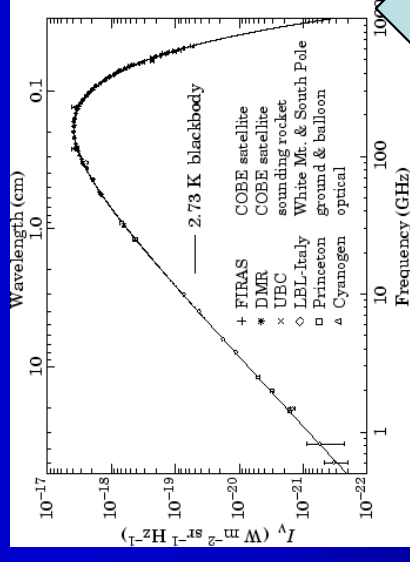
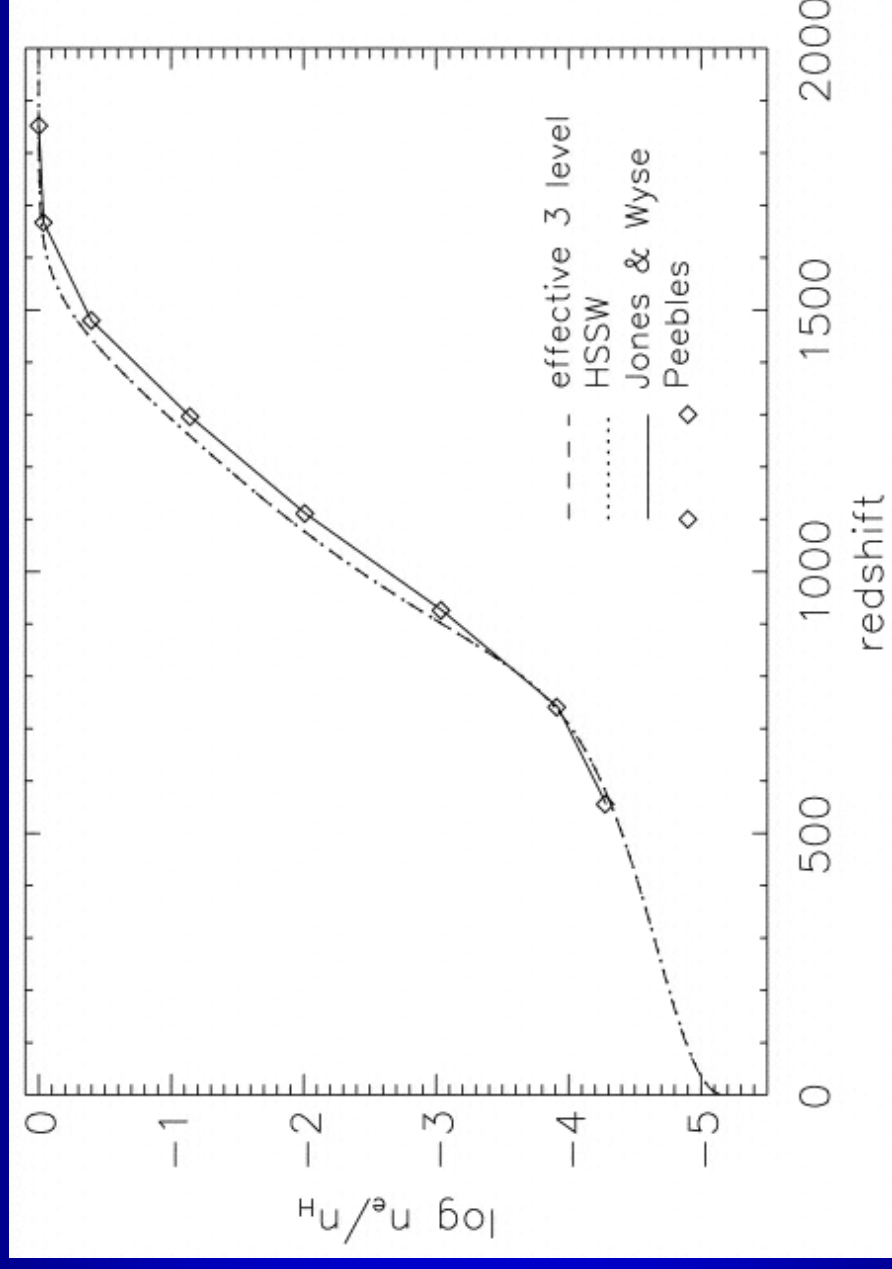


FIG. 1.—Spectrum of the Primeval Fireball radiation as it would be observed now is shown for a purely thermal spectrum (curve 1), taking account of the redshifted ionizing recombination radiation (curve 2), and taking account of the redshifted resonance line radiation (curve 3). The dashed curve (4) shows the separate contribution due to two-quantum decay. The curves are computed for the flat cosmological model.



The problem is that in this spectral region, dust emission dominates (CIB).

# How the Universe became neutral? (III)

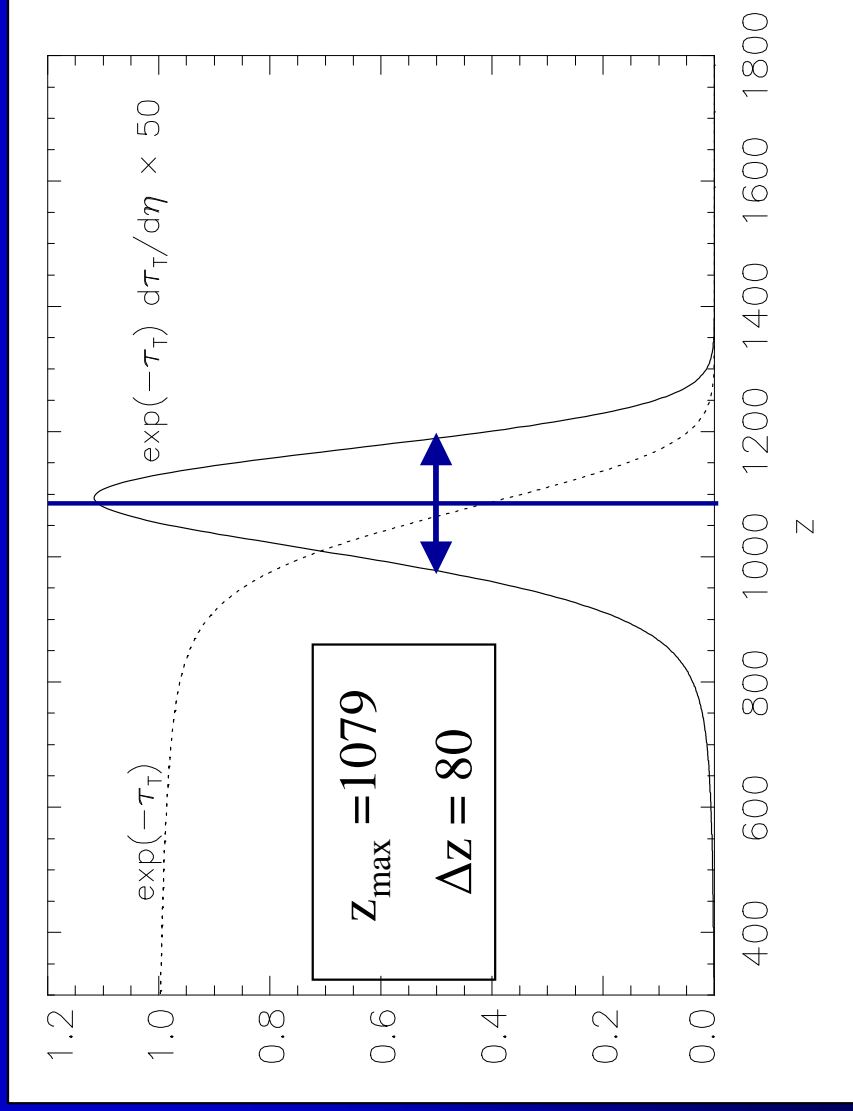


- Zel'dovich, Kurt & Sunyaev (1968)
- Peebles (1968)
- Lyubarsky & Sunyaev (1983)
- Jones & Wyse (1985)
- Hu et al. (1995, HSSW)
- Seager, Sasselov & Scott (1999, 2000).

This curve is a key ingredient to predict the angular power spectrum of the CMB, because it directly gives the fraction of free electrons.

# The (Thomson) visibility function

Prior to the recombination epoch, the photons and the electrons are tightly coupled due to Thomson scattering. When the number density of electrons decreases, the photons are released and the CMB is formed.



- The relevant quantity is the Thomson optical depth.

$$\tau = \int \sigma_T n_e dl$$

- The **visibility function** gives the probability that a photon observed now was last scattered at redshift  $z$ :

$$V = \exp(-\tau) \frac{d\tau}{d\eta}$$

# Recombination. Basic equations

1. The radiation field. Given by the **radiative transfer equation**. For an homogeneous and isotropic (I -> J) expanding medium:

$$\begin{aligned}\frac{dJ(\nu, t)}{dt} &= \frac{\partial J(\nu, t)}{\partial t} - \nu H(t) \frac{\partial J(\nu, t)}{\partial \nu} \\ &= -3H(t)J(\nu, t) + c[j(\nu, t) - \kappa(\nu, t)J(\nu, t)],\end{aligned}$$

This equation is in its most general form and is difficult to solve, but we can do two assumptions:

- The spectral distortions are very small (FIRAS: Fixsen et al. 1996, showed that  $\Delta I/I_0 < 10^{-4}$ ). Thus,  $J(\nu, t) = B(\nu, t)$ .
- Quasi-static solution for spectral-line profile is valid (Rybicki & Dell'Antonio 1994). We can use the Sobolev escape probability method to deal with the evolution of all lines.

# Basic equations (II)

## 2. The rate equations.

$$a(t)^{-3} \frac{d[n_i(t)a(t)^3]}{dt} = [n_e(t)n_c(t)P_{ei} - n_i(t)P_{ic}] + \sum_{j=1}^N [n_j(t)P_{ji} - n_i(t)P_{ij}],$$

- Collisional rates are of minor importance (Peebles 68, Seager et al. 2000).
- Photoionization/Photorecombination **radiative** rates are computed by integrating the blackbody radiation field, e.g.

$$R_{ic} = 4\pi \int_{\nu_0}^{\infty} \frac{\sigma_{ic}(\nu)}{h_P \nu} J(\nu, t) d\nu.$$

$$\sum_{i>1}^N n_e n_c R_{ci} = n_e n_c \sum_{i>1}^N \left( \frac{n_i}{n_e n_c} \right)^{\text{LTE}} 4\pi \int_{\nu_0}^{\infty} \frac{\sigma_{ic}(\nu)}{h_P \nu} \times \left( \frac{2h_P \nu^3}{c^2} + B(\nu, T_R) \right) e^{-h_P \nu/k_B T_M} d\nu.$$

# Basic equations (III)

3. Sobolev escape probability method. The net bound-bound rate is:

$$\Delta R_{ji} = p_{ij} \{ n_j [A_{ji} + B_{ji} B(v_{ij}, t)] - n_i B_{ij} B(v_{ij}, t) \} .$$

The escape probability  $p_{ij}$  encodes the probability that photons associated to the considered transition will “escape” without being further scattered or absorbed. The concept is similar to stellar atmospheres.

In this case, it can be shown that (Seager et al. 2000; Dubrovich & Grachev 2004)

$$\tau_s = \frac{A_{ji} \lambda_{ij}^3 [n_i (g_j/g_i) - n_j]}{8\pi H(z)} .$$

$$p_{ij} = \frac{1 - \exp(-\tau_s)}{\tau_s} .$$

# Basic equations (IV)

4. Matter temperature evolution (Compton cooling + adiabatic expansion)

$$(1+z) \frac{dT_M}{dz} = \frac{8\sigma_T U}{3H(z)m_e c} \frac{n_e}{n_e + n_H + n_{He}} \times (T_M - T_R) + 2T_M$$

5. Other equations.
  1. Hubble constant evolution
  2. Helium recombination.

# Recombination. Status of the art (I)

- After ZKS68 and P68, many authors have refined the computation of the recombination process, based on the effective 3-level atom model (e.g. Jones & Wyse 1985).
- To solve the complete set of ODEs (ordinary differential equations) is computationally difficult. The problem is very stiff, and the accuracy requirements are very high.
- If one is not interested in the lines, but in the total electron fraction, the accuracy requirements can be relaxed.
- In addition, one can assume statistical equilibrium between the l-substates, i.e. that the sublevels are populated according to  $N(n,l)=(2l+1) N(n,l=0)$ . This is not obvious for the cosmological recombination, where collisions are not important.
- Best determination to date: Seager, Sasselov & Scott (1999, 2000), used a 300-level hydrogen atom (statistical equilibrium between l-substates assumed). This is the **RECFAST** code. Focused on  $n_e$ .

# Recombination. Status of the art (II)

- Dubrovich (1975) proposed to look for spectral distortions for higher transitions.

- Du
- Ma
- 2003
- equa
- the l

Lupenko et al.  
I with the  
amplitude of

onio 1993), but

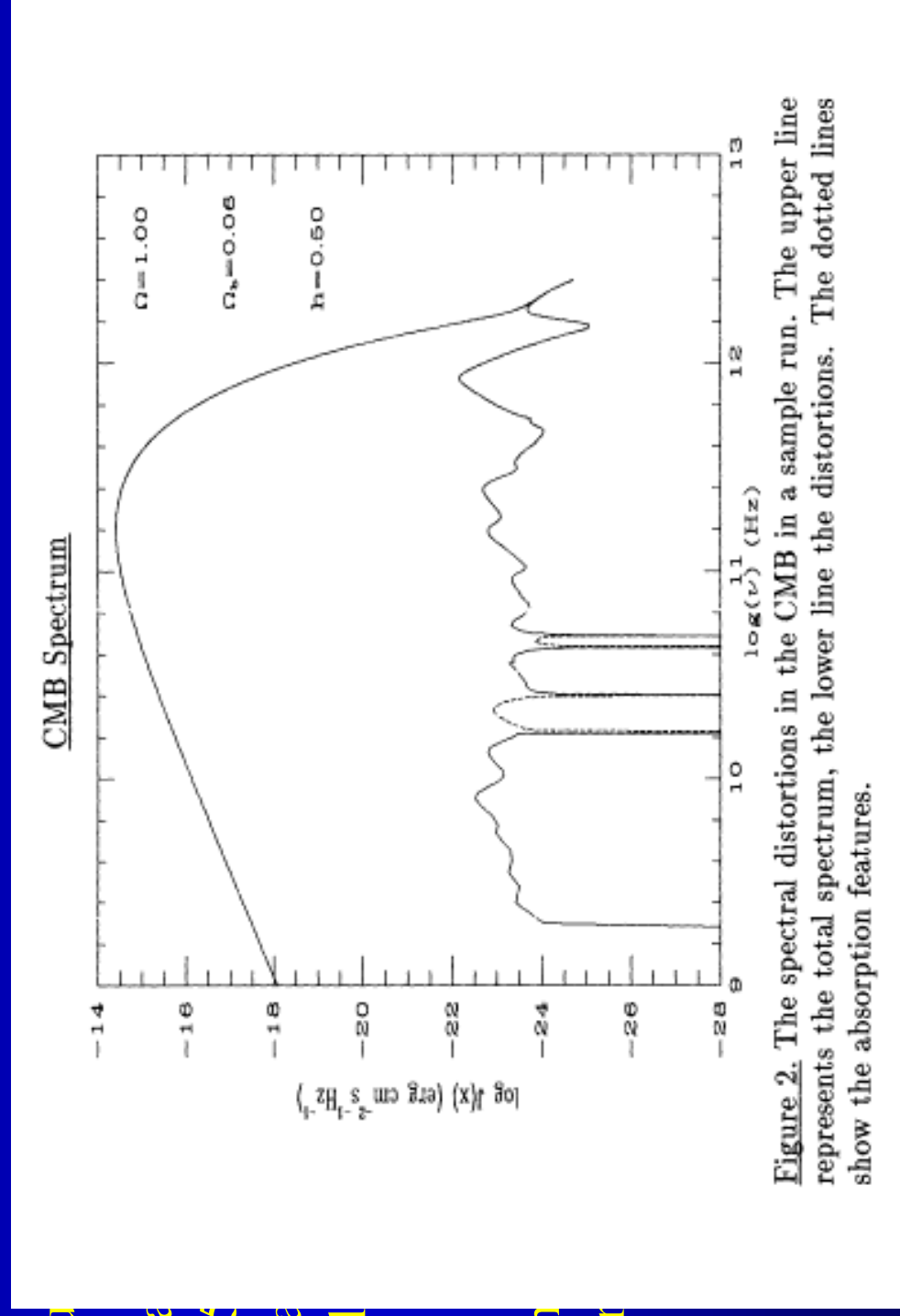


Figure 2. The spectral distortions in the CMB in a sample run. The upper line represents the total spectrum, the lower line the distortions. The dotted lines show the absorption features.

- On
- the r

# **Our work: how to observe spectral features from the epoch of recombination**

- **Frequency Spectrum.** We have computed the spectral distortions to the blackbody arising from H recombination in the frequency range 1- 3500 GHz.
- **Resonant (coherent) scattering of CMB photons.** Use angular fluctuations and observations at different frequencies.

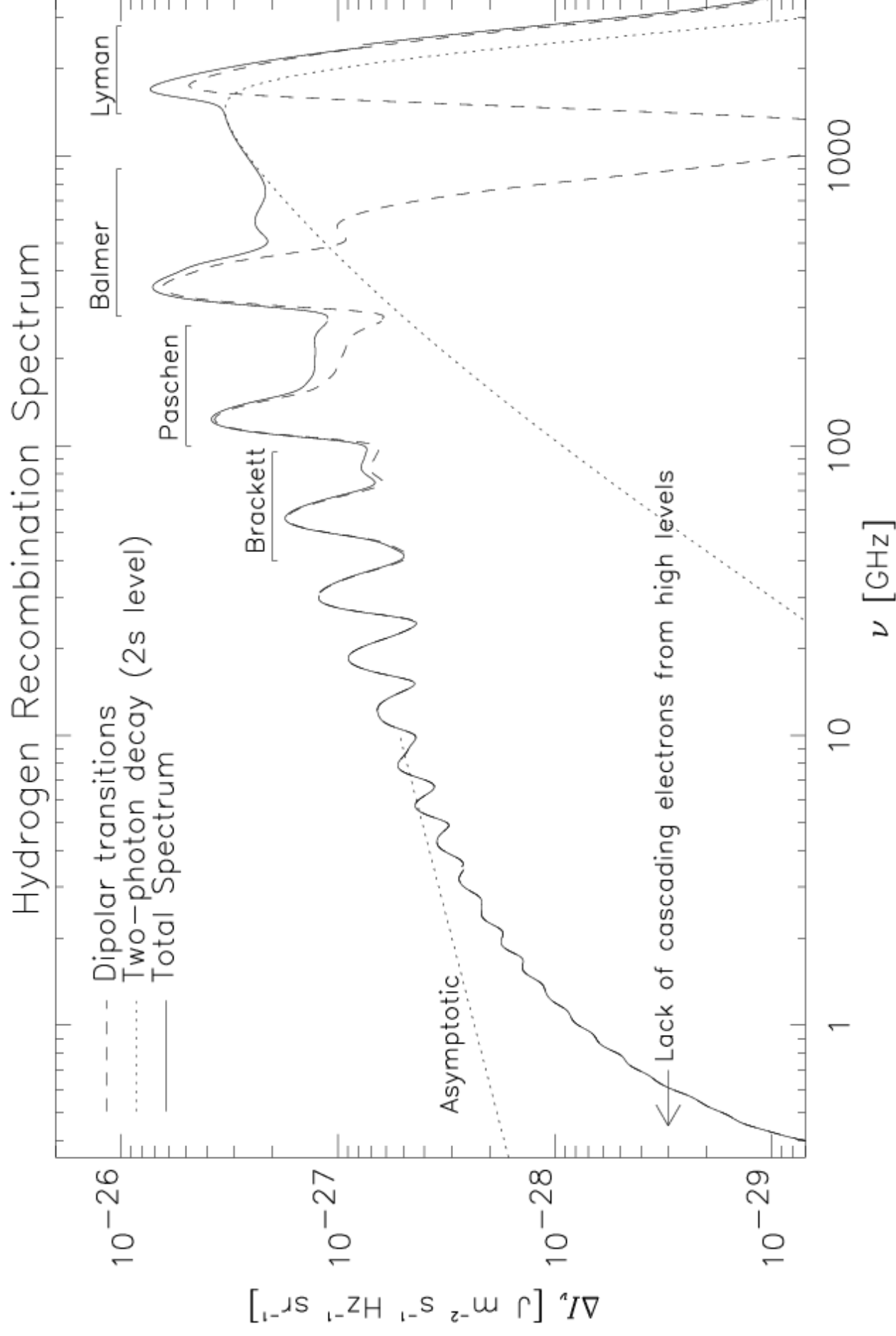
# Hydrogen Recombination Spectrum

(Rubio-Martín, Chluba & Sunyaev 2006 MNRAS accepted, astro-ph/0607373)

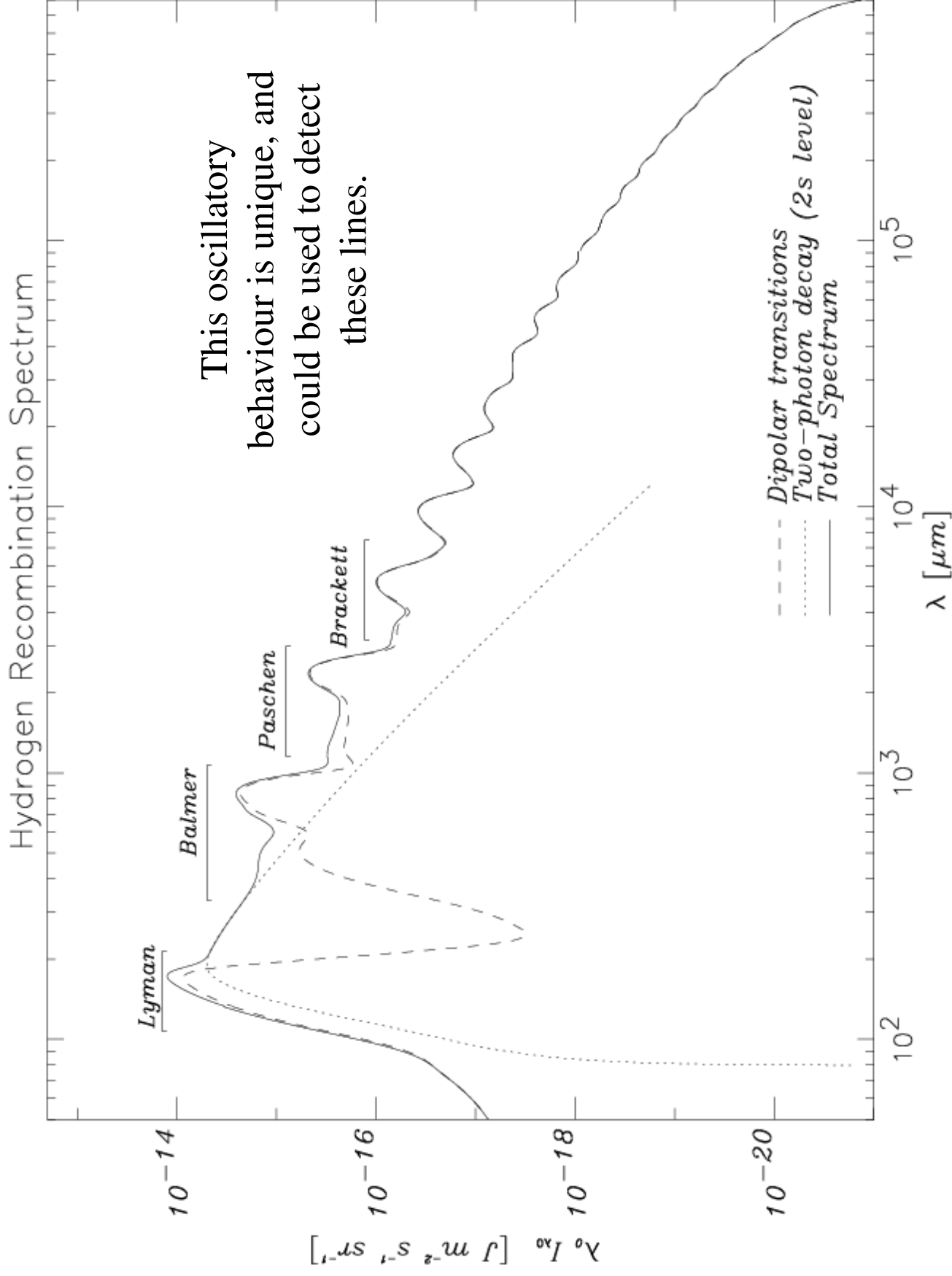
- All states (including angular momentum sublevels) treated in detail up to  $n=30$ . Thus, 465 levels are solved simultaneously for the hydrogen atom. (We use a variable-order, variable-step method implementing the backward differentiation formulae).
- Integration range in redshift: [500, 3500]
- Spectral distortion due to the 2s two photon decay included.
- Lines (bound-bound transitions) are computed as:

$$\Delta I_{ij}(\nu) = \frac{ch}{4\pi} \frac{\Delta R_{ij}(z_{em})}{H(z_{em}) [1 + z_{em}]^3},$$

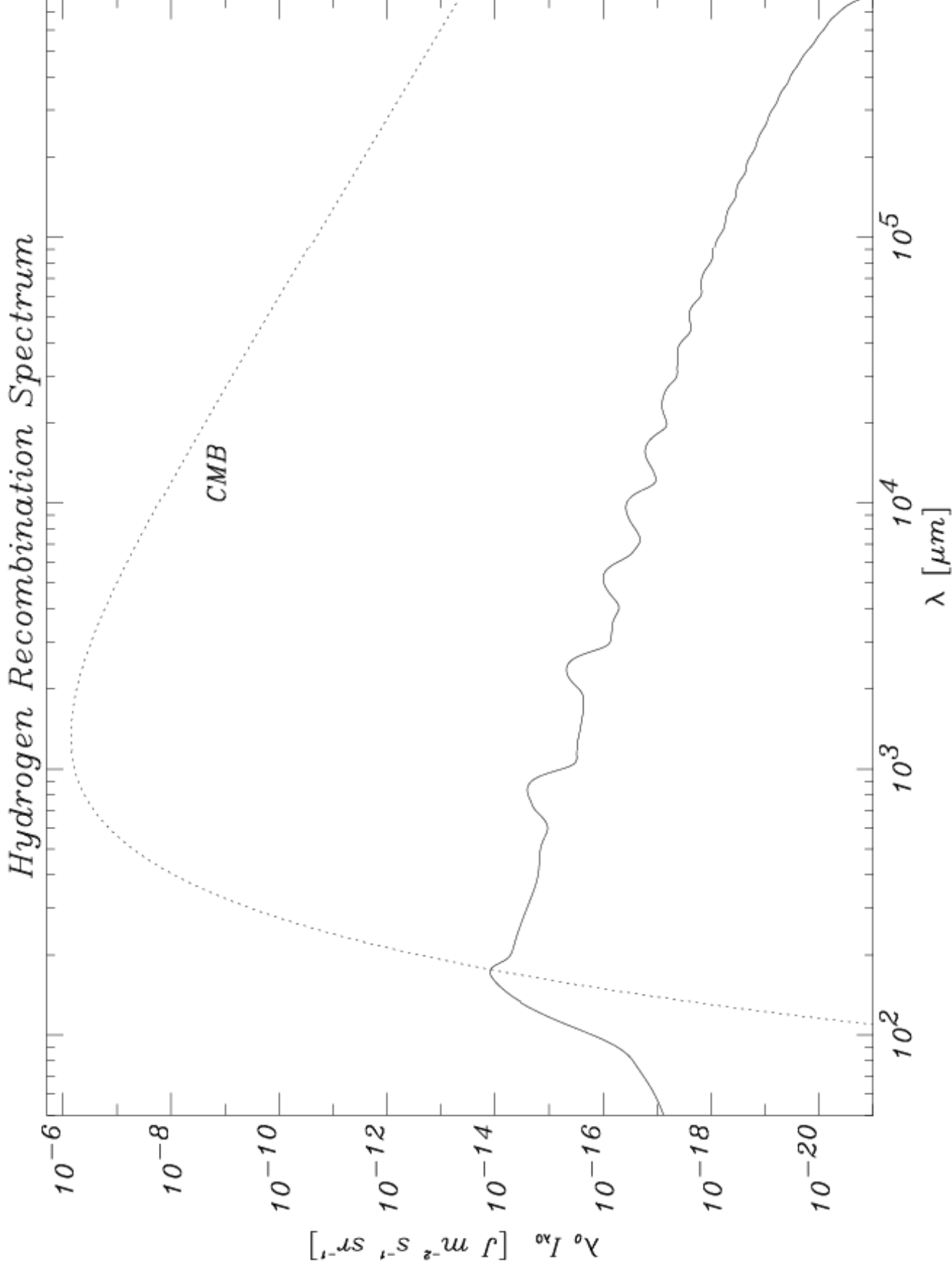
# Hydrogen Recombination Spectrum



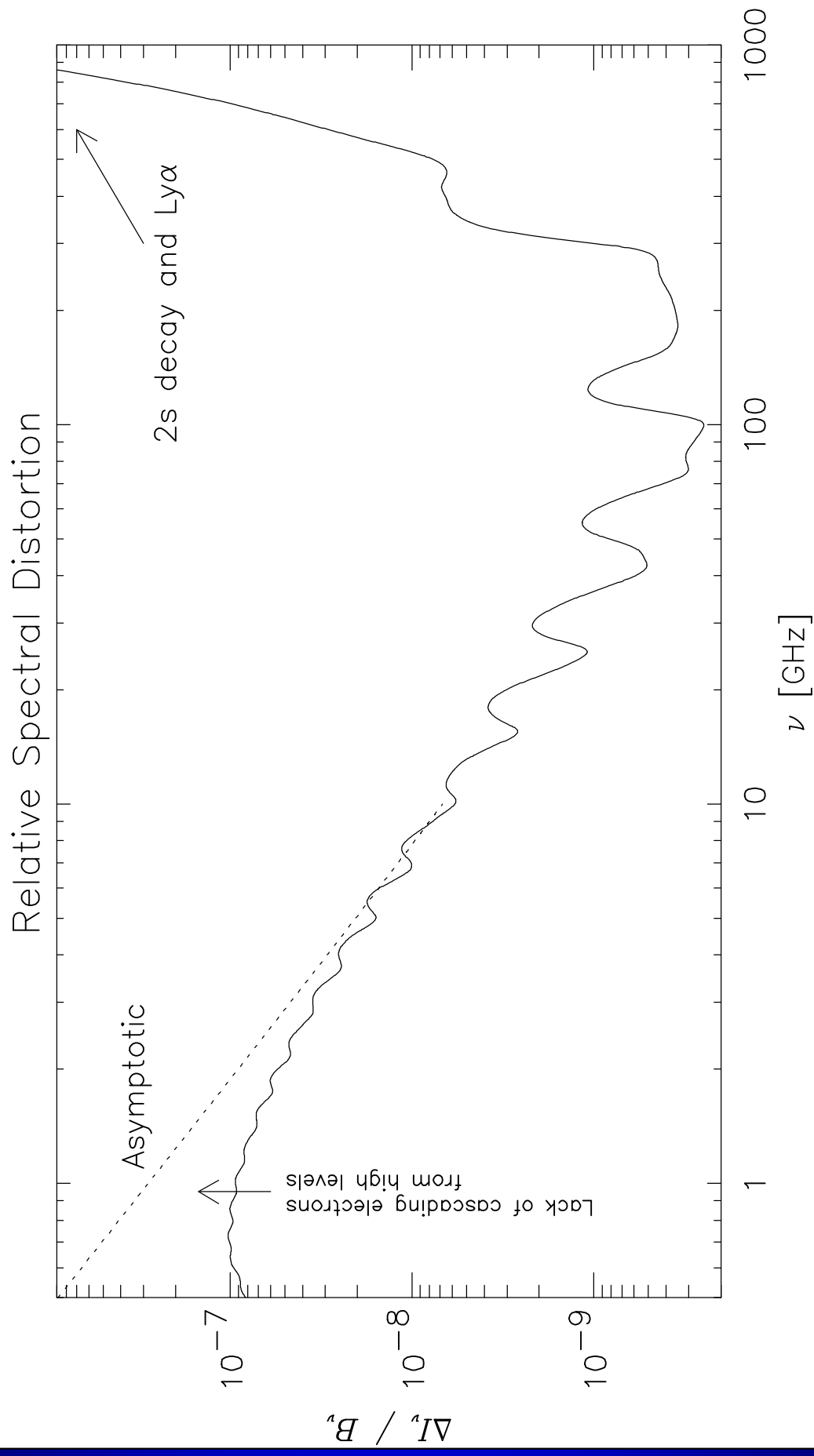
# ... Or in wavelengths



# Relative intensity of the lines



# Relative intensity of the lines



# Positions and widths of the features

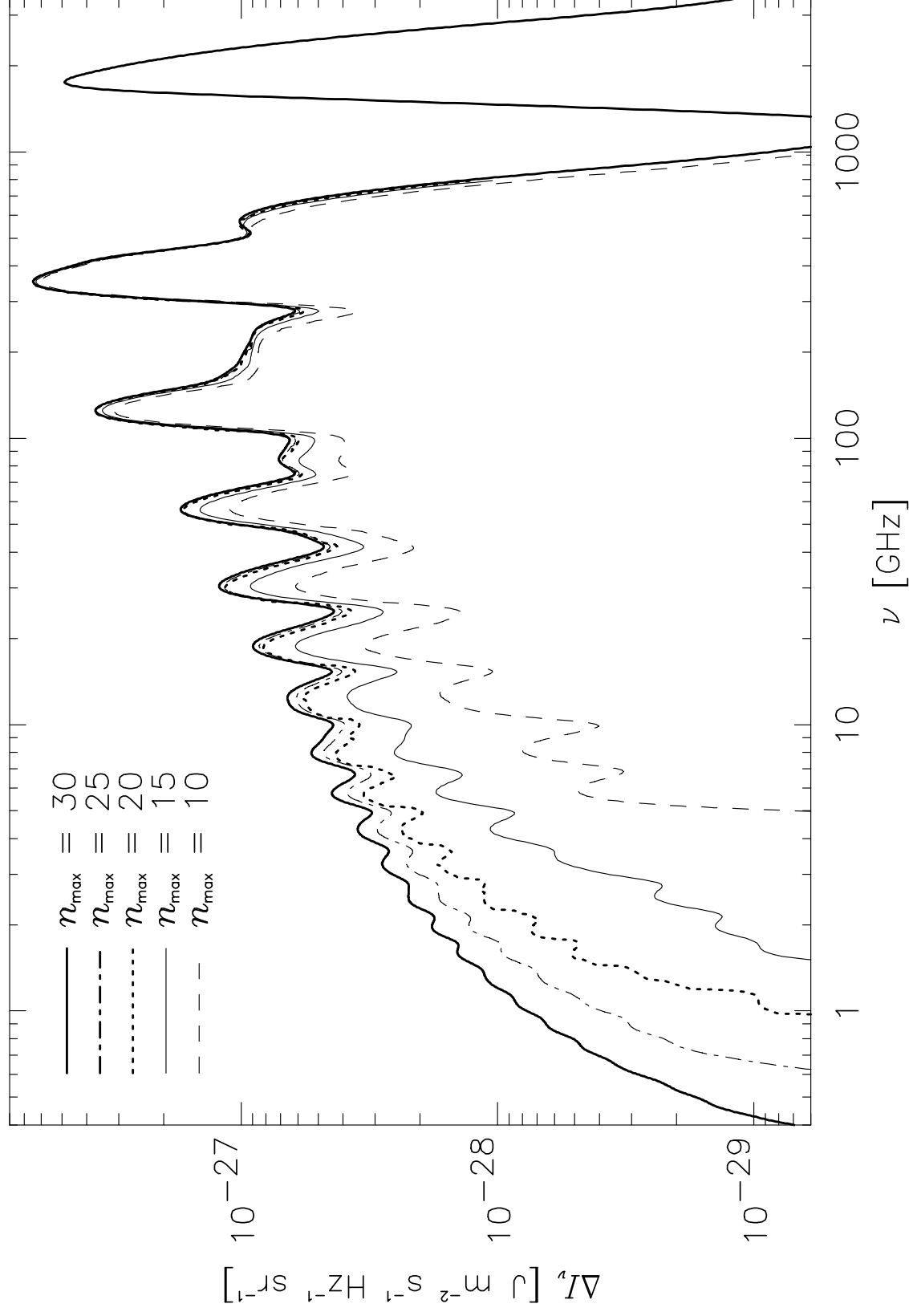
6 *J. A. Rubiño-Martín, J. Chluba & R. A. Sunyaev*

**Table 1.** Positions and amplitudes of the main features shown in Fig. 1. We show the central frequency ( $\nu_0$ ) and wavelength ( $\lambda_0$ ) as observed today, the relative width at half maximum ( $\Delta\nu/\nu$ ) and the peak intensity for the features corresponding to the first five series of hydrogen. For comparison, the last five columns show the central redshift of formation, the central frequency, the relative width, the peak and relative amplitude of the corresponding  $\alpha$ -transition (i.e.  $\Delta n = 1$ ) when considered separately.

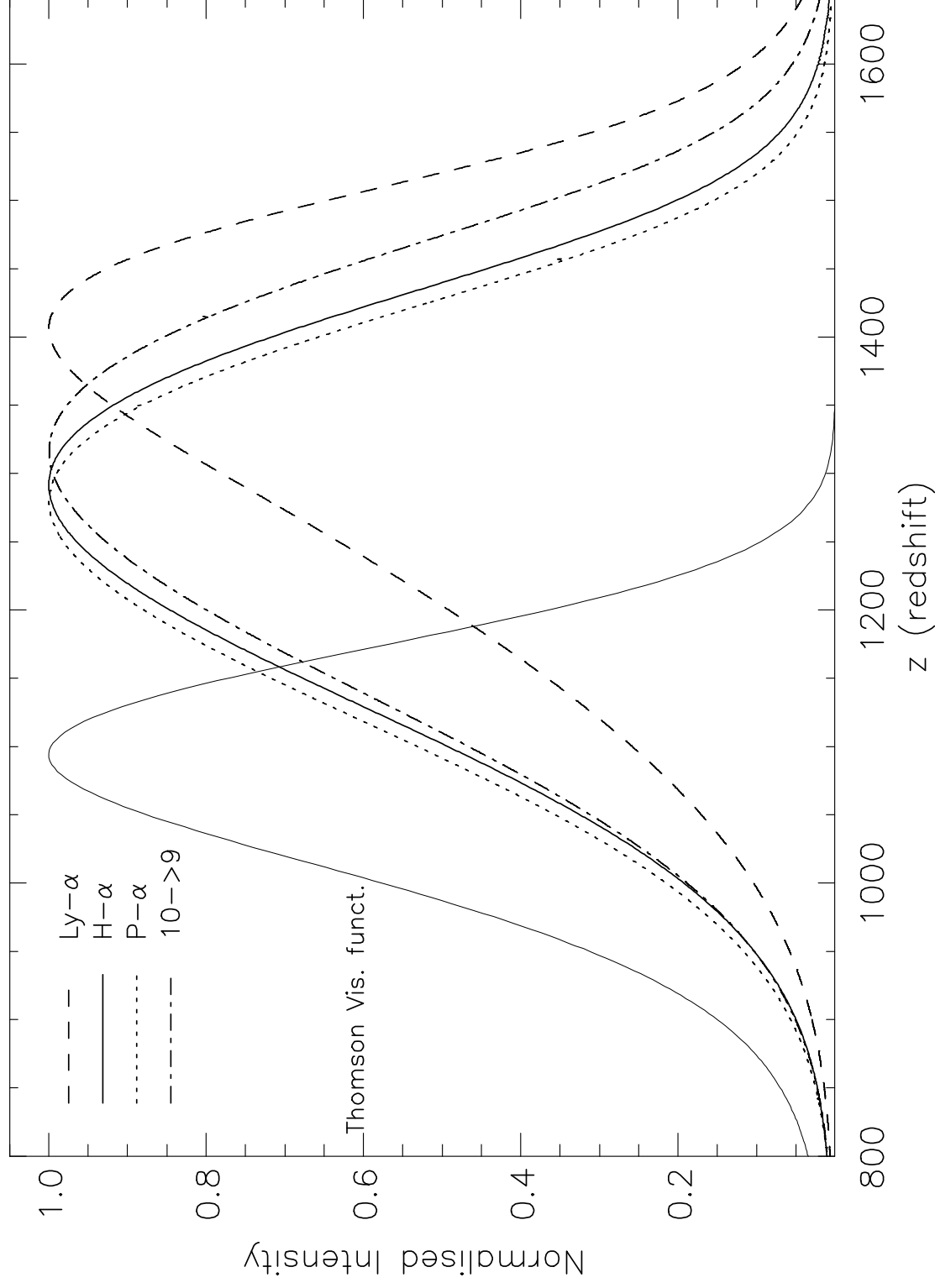
Series	$n$	$\nu_0$ [GHz]	$\lambda_0$ [ $\mu\text{m}$ ]	$\Delta\nu/\nu$	$\Delta I_\nu(\text{peak})$ [ $\text{J m}^{-2} \text{s}^{-1} \text{Hz}^{-1} \text{sr}^{-1}$ ]	$z_\alpha$	$\nu_\alpha$ [GHz]	$(\Delta\nu/\nu)_\alpha$	$\Delta I_\alpha$ [ $\text{J m}^{-2} \text{s}^{-1} \text{Hz}^{-1} \text{sr}^{-1}$ ]	$\Delta I_\alpha/\Delta I_\nu$ [%]
Lyman	1	1732	175	0.28	$7.4 \times 10^{-27}$	1407	1752	0.23	$4.8 \times 10^{-27}$	65
Balmer	2	353	844	0.37	$7.2 \times 10^{-27}$	1274	358	0.26	$6.5 \times 10^{-27}$	93
Paschen	3	125	2390	0.31	$3.8 \times 10^{-27}$	1259	127	0.26	$3.3 \times 10^{-27}$	87
Brackett	4	56	5350	0.36	$1.8 \times 10^{-27}$	1304	57	0.27	$1.2 \times 10^{-27}$	67
Pfund	5	30	9993	0.39	$1.2 \times 10^{-27}$	1312	31	0.27	$7.3 \times 10^{-28}$	61

They are broad features. Electron broadening is not changing this picture.

# Convergence of the result

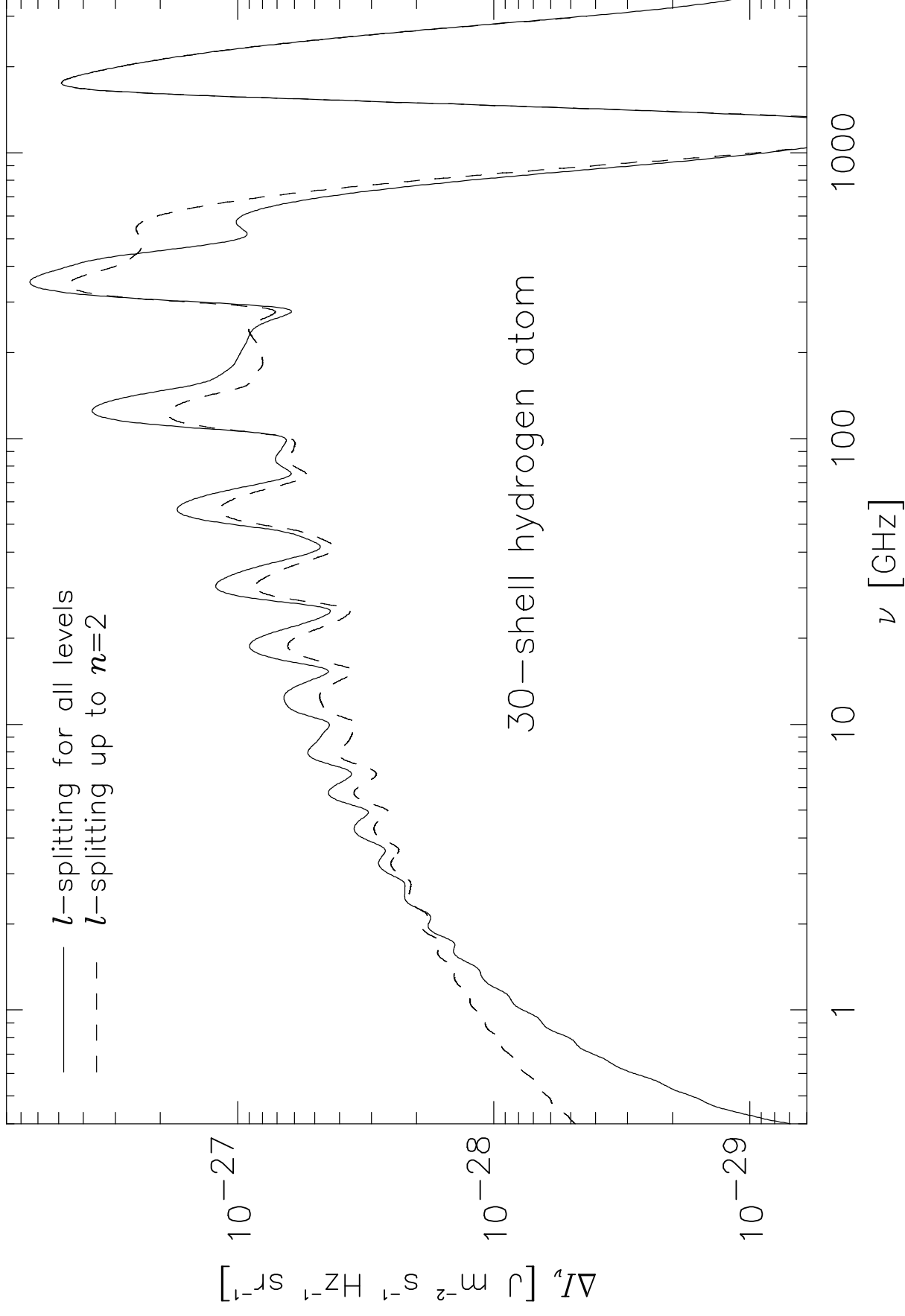


# Redshift of formation of the lines

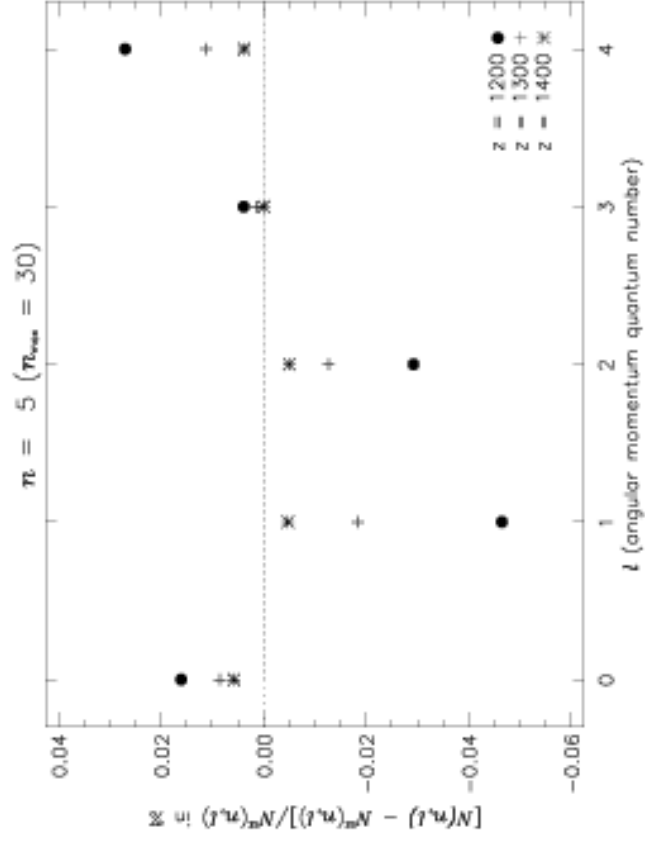
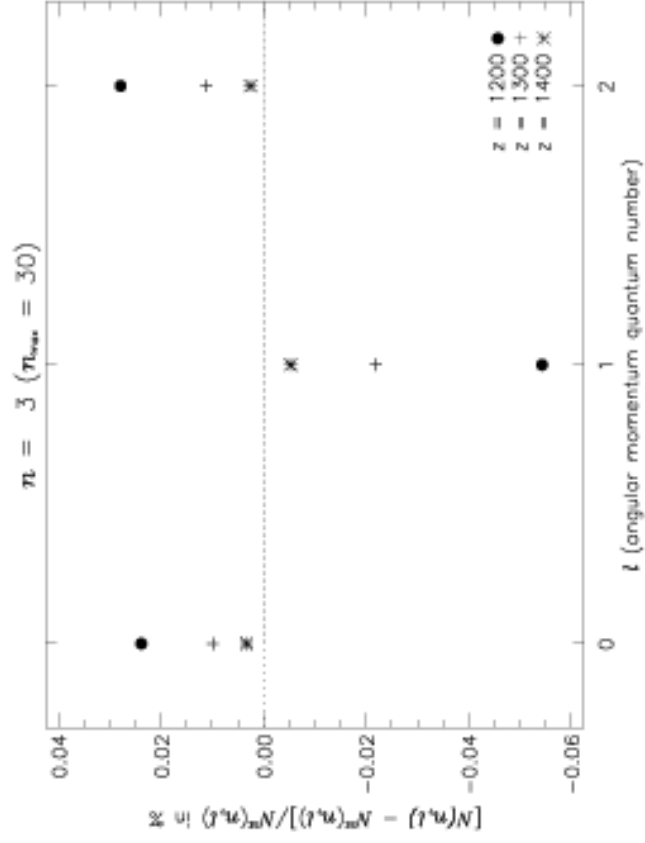
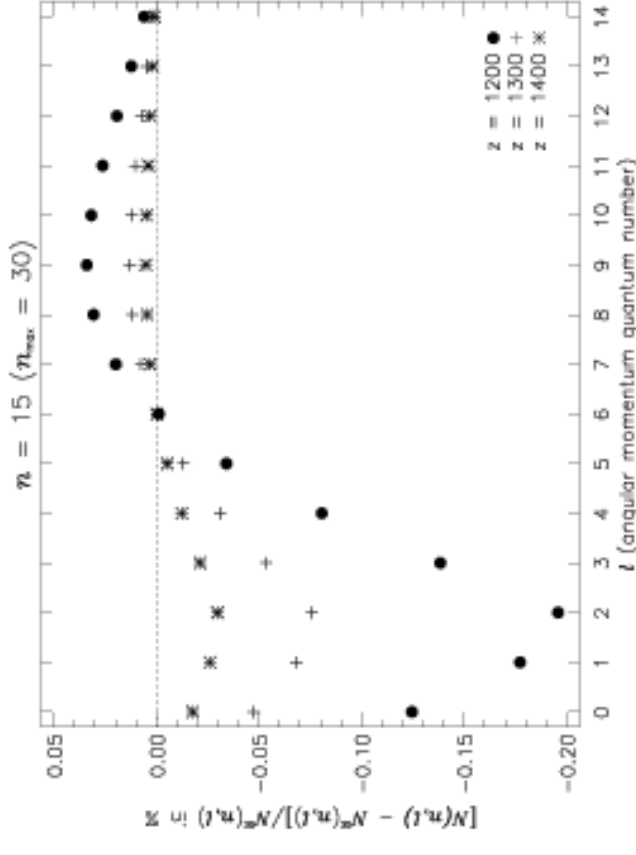
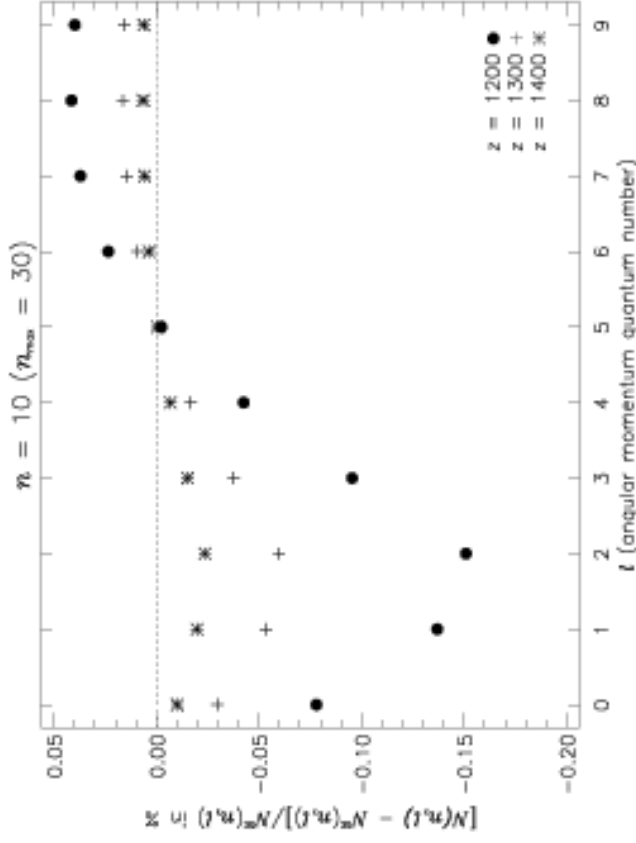


Lines are formed prior to the epoch of recombination

# Importance of detailed $l$ -treatment



# Importance of detailed l-treatment



# Impact on the residual electron fraction

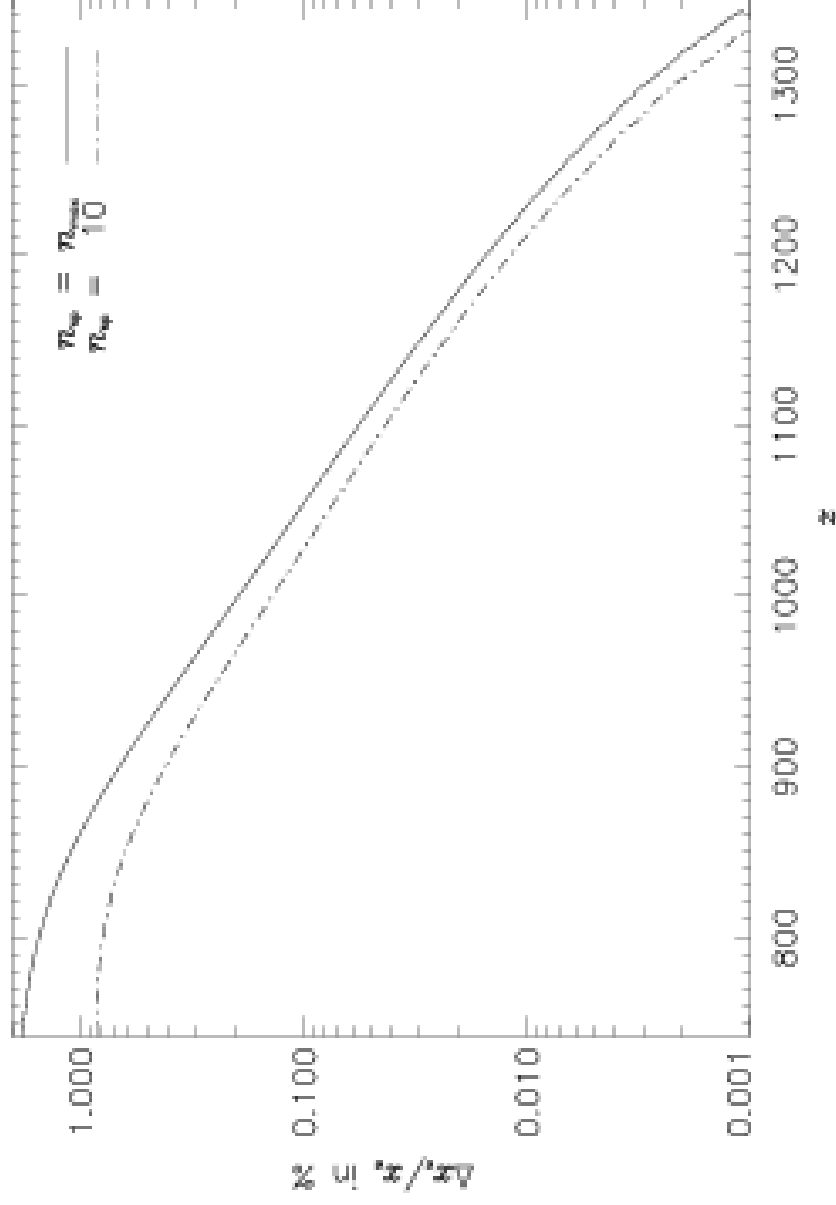
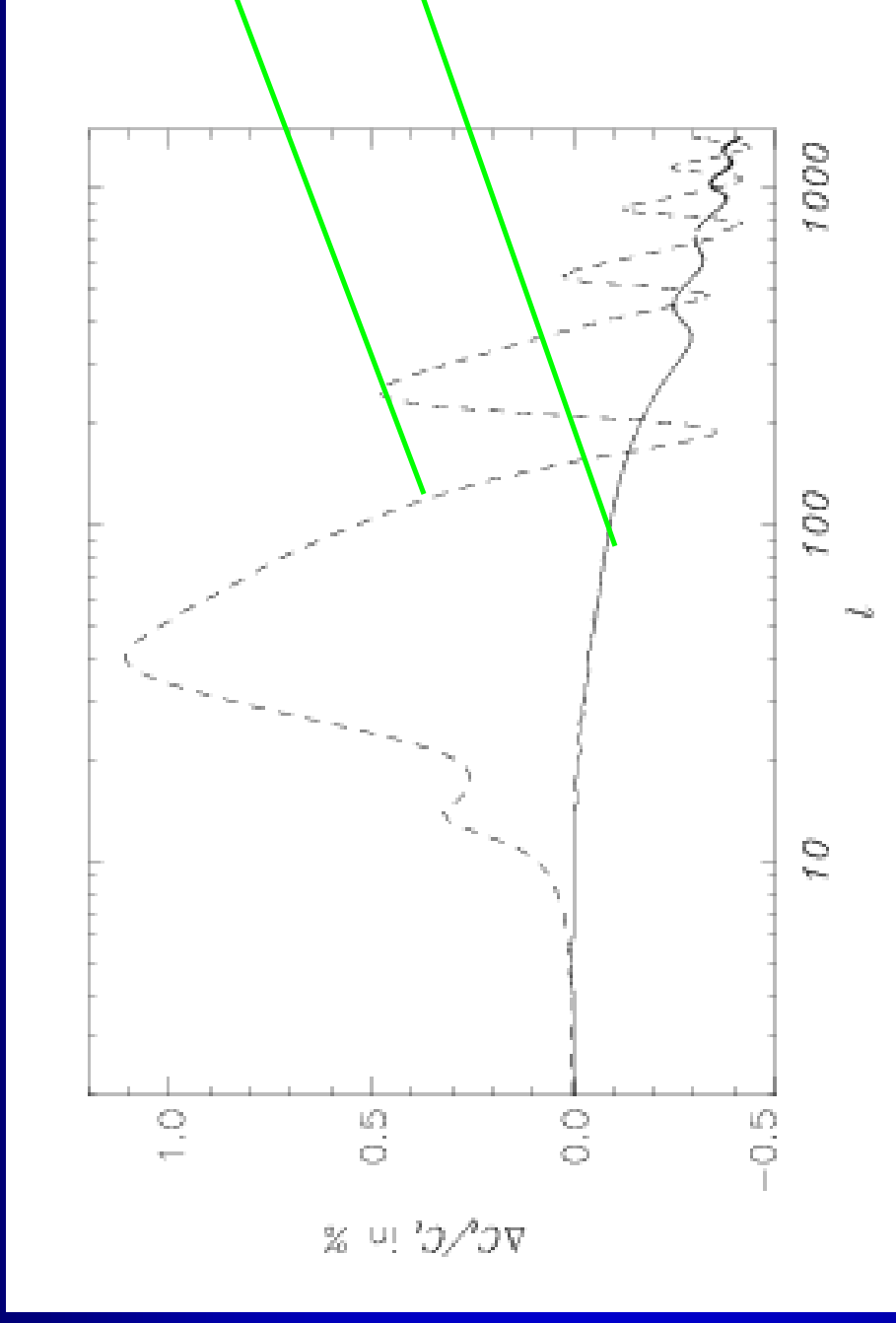


**Figure 14.** Relative change in the free electron fraction ( $x_e = N_e/N_H$ ). We consider the 25-shell atom and show the relative difference in  $x_e$  with respect to the standard computation ( $\Delta x_e/x_e \equiv [x_e - x_e(n_{sp} = 2)]/x_e(n_{sp} = 2)$ ) for two cases: full computation ( $n_{sp} = n_{max}$ ) and  $n_{sp} = 10$ .

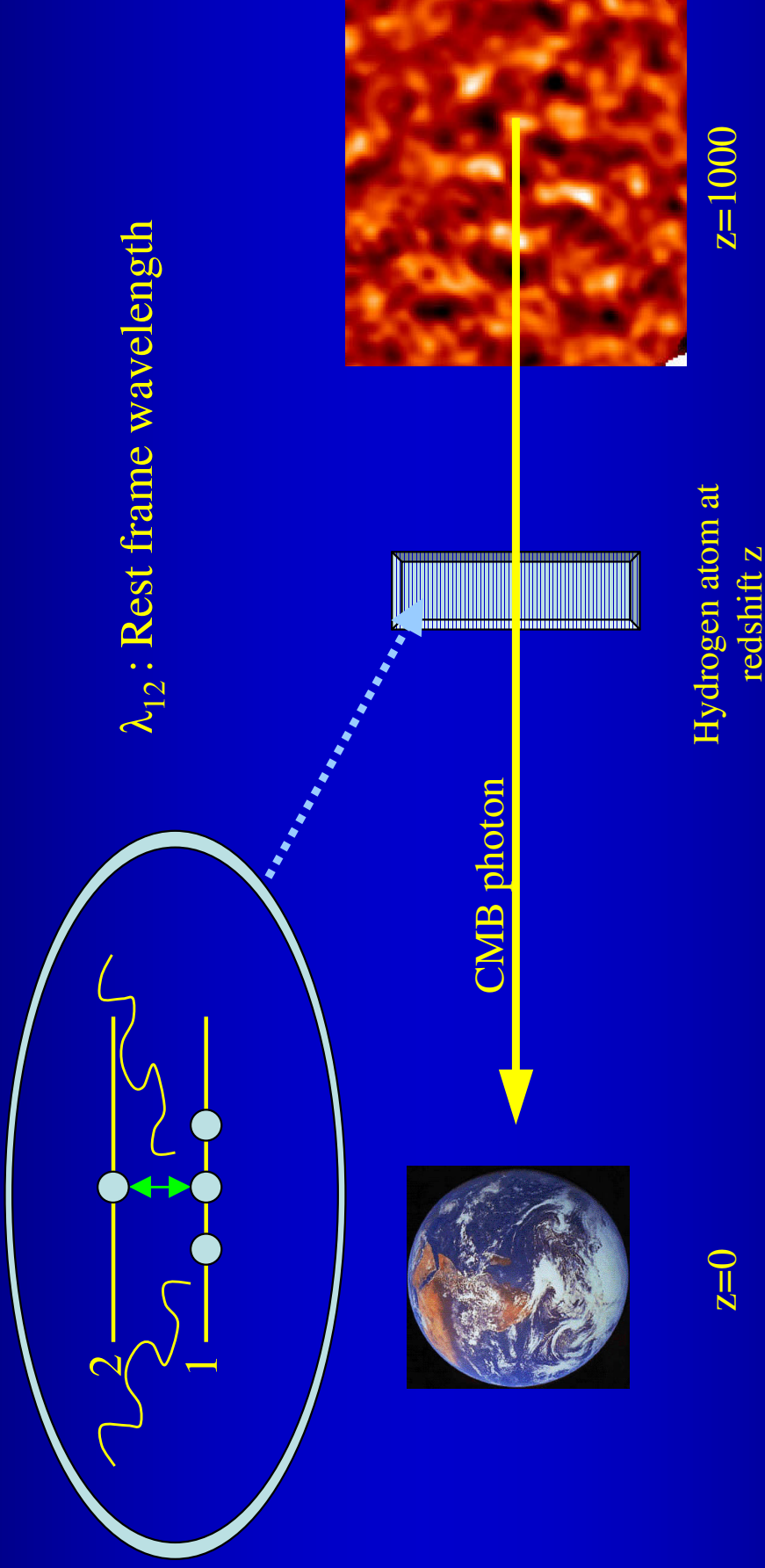
# Effect of the $l$ -treatment in the $C_l$ s



- The effect is larger at low redshifts. The net (integrated) effect on the power spectrum is of the order of 1%.
- New paper in preparation including  $n=100$  shells, plus detailed treatment of collisions.

# Coherent scattering of the CMB photons

(Rubio-Martín, Hernández-Monteagudo & Sunyaev 2005 A&A 438, 461)

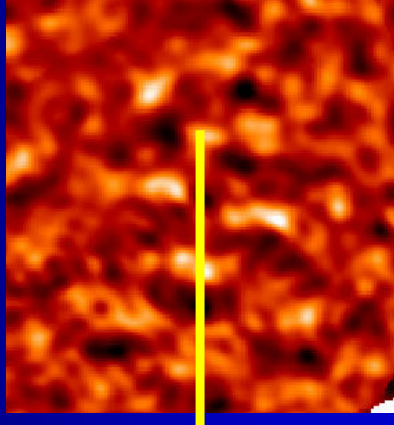


$$\frac{\Delta T}{T_0}(\theta) = e^{-\tau_\nu} \left. \frac{\Delta T}{T_0}(\theta) \right|_{orig.} + \left. \frac{\Delta T}{T_0}(\theta) \right|_{new}$$

$\lambda_{12}(1+z)$   $\longleftrightarrow$   $\lambda_{12}$

# Coherent scattering of the CMB photons

(Rubino-Martín, Hernández-Monteagudo & Sunyaev 2005)

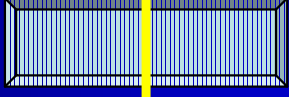


$z=1000$



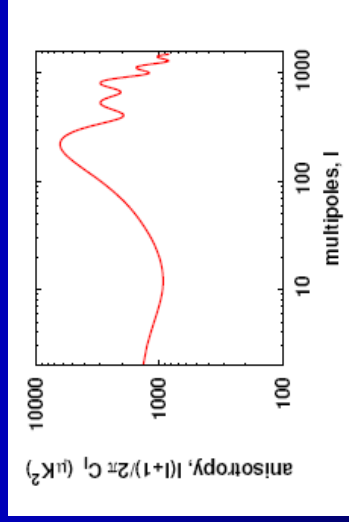
$z=0$

CMB photon

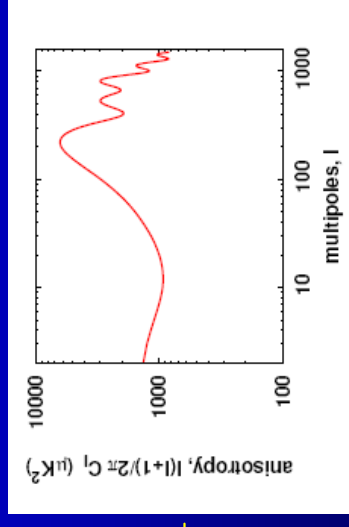


Hydrogen atom at redshift  $z$

$$\lambda_{12}(1+z) \quad \longrightarrow \quad \lambda_{12}$$



$C_l + \delta C_l$

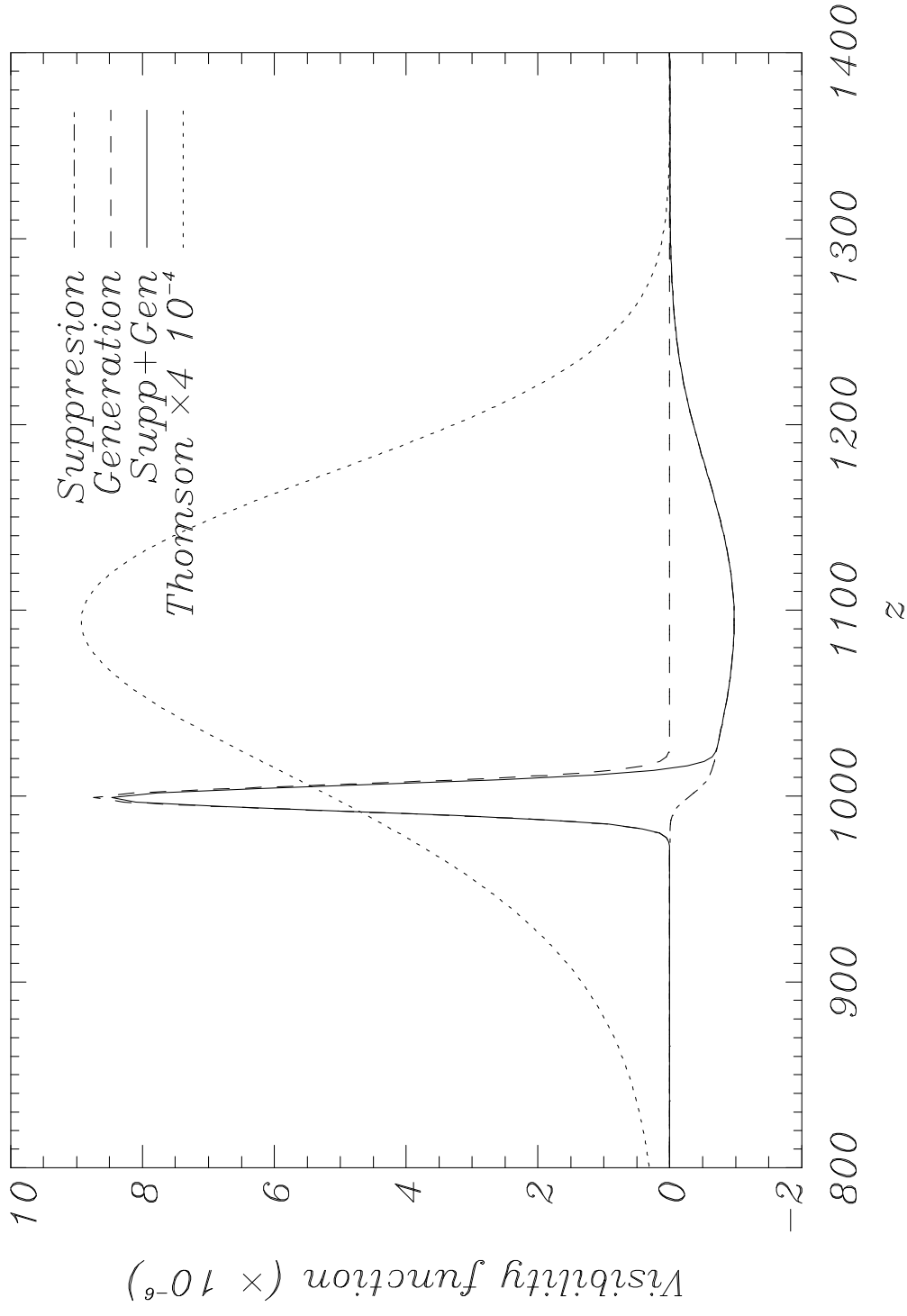


$C_l$

$$\delta C_l = \tau_{\text{RPM}} \cdot C_l(\ell) + \tau_{\text{RPM}}^2 \cdot C_2(\ell) + O(\tau_{\text{RPM}}^3)$$

(Basu et al. 2005)

# Coherent scattering of the CMB photons



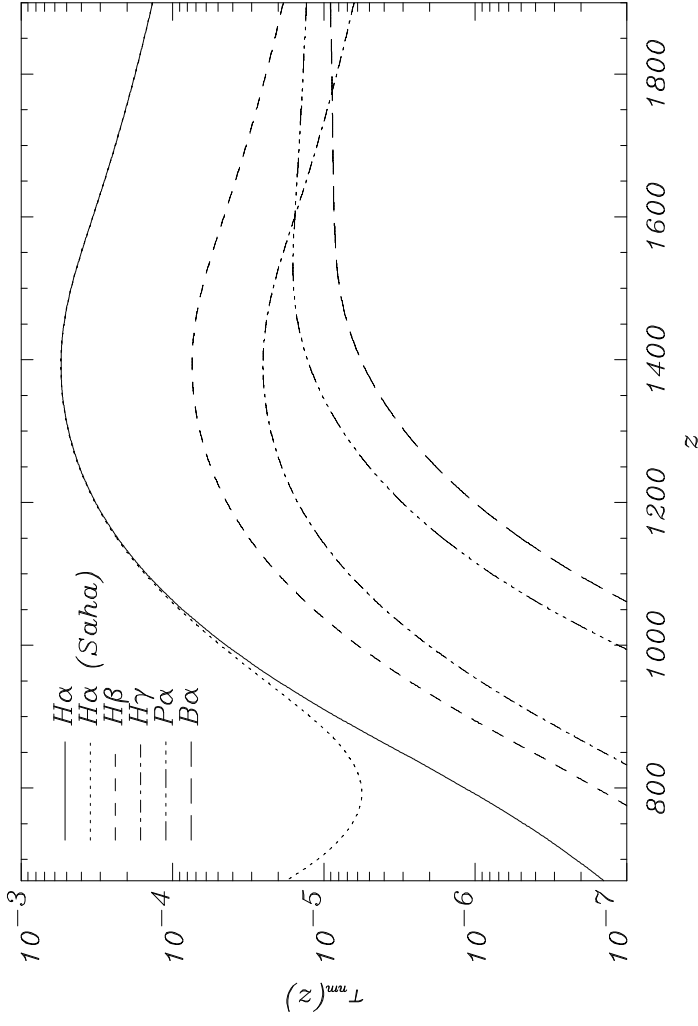
# Computing the change in the $C_l$

- Compute the optical depth for the line of interest.
- Compute the linear term using an standard Boltzmann code to integrate the CMB anisotropies (CMBFAST)

$$\delta C_l = \tau_{\text{FRM}} \cdot C_l(\ell) + \tau_{\text{FRM}}^2 \cdot C_2(\ell) + O(\tau_{\text{FRM}}^3)$$

- To observe the effect, we compare power spectra at two frequencies:

$$\delta C_l = C_l(\text{with line}) - C_l(\text{without line})$$



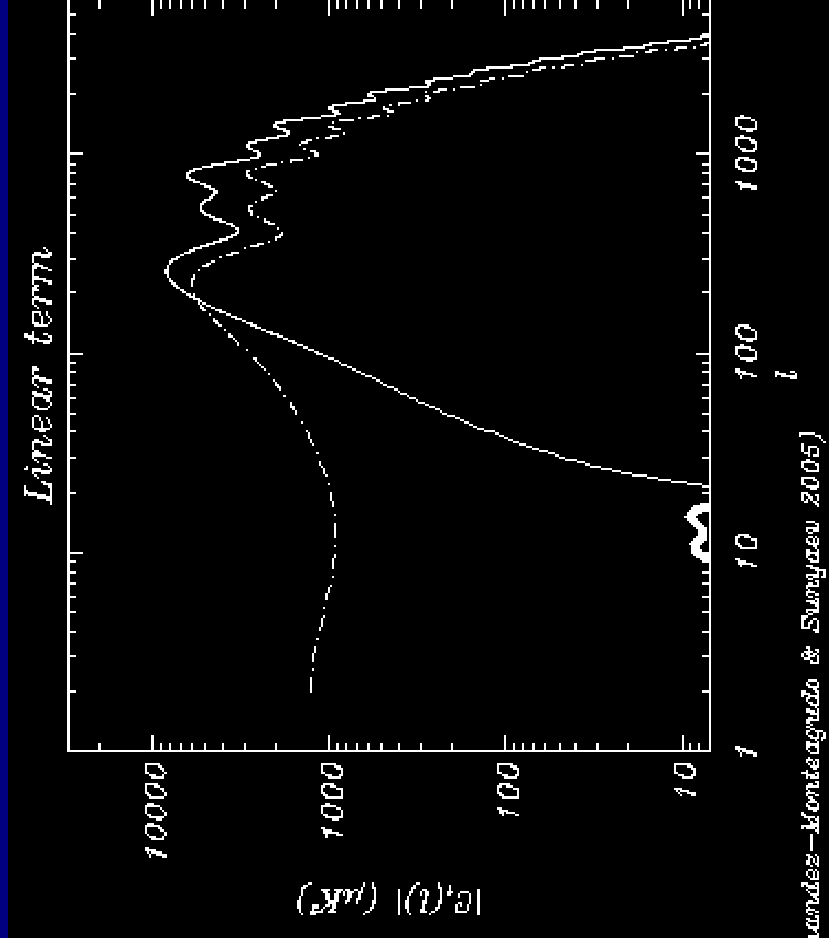
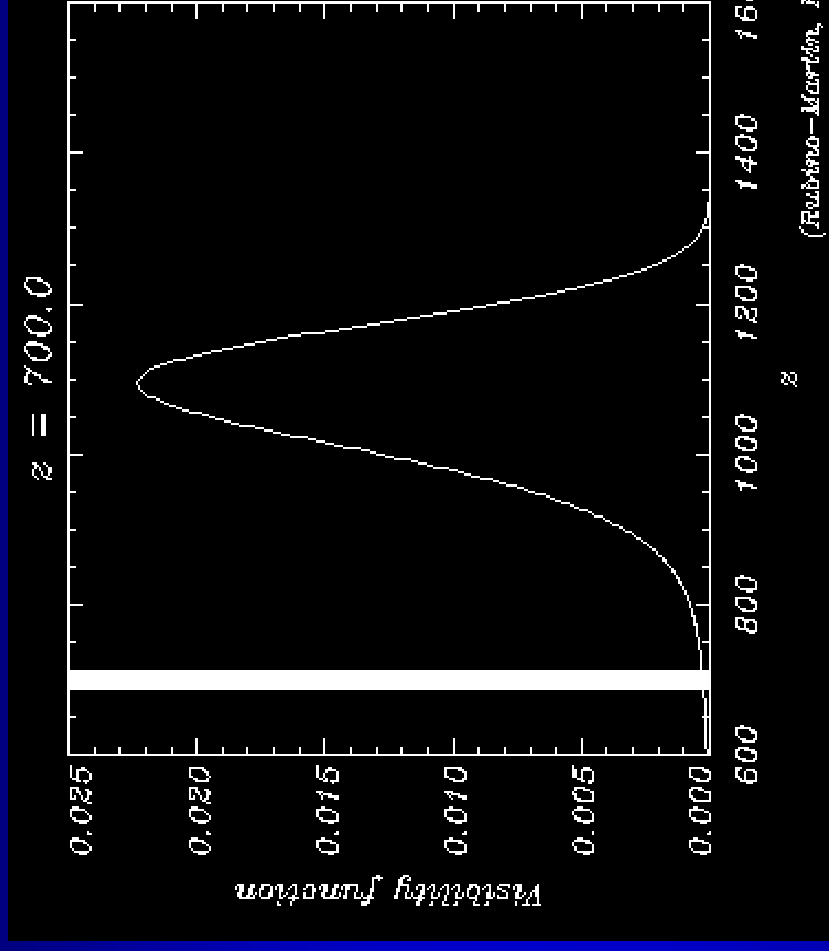
# Computations for this work

- All states (including angular momentum sublevels) treated in detail up to  $n=10$ .
- Optical depths for the main transitions: all very small.

Transition	$m$	$\lambda_{nr}$ (Å)	$f_{nr}$	$\nu_\alpha(z=1000)$ (GHz)	$\tau_{nr}(z=1000)$
<b>Balmer lines (<math>n=2</math>)</b>					
H $\alpha$	3	6562.8	0.6407	456.3	$4.53 \times 10^{-5}$
H $\beta$	4	4861.3	0.1193	616.1	$6.14 \times 10^{-6}$
H $\gamma$	5	4340.5	0.0447	690.0	$2.09 \times 10^{-6}$
<b>Paschen lines (<math>n=3</math>)</b>					
P $\alpha$	4	18751.0	0.8421	159.7	$1.17 \times 10^{-7}$
P $\beta$	5	12818.1	0.1506	233.6	$1.47 \times 10^{-8}$
P $\gamma$	6	10938.1	0.0558	273.8	$4.75 \times 10^{-9}$
<b>Brackett lines (<math>n=4</math>)</b>					
B $\alpha$	5	40512.0	1.0377	73.9	$2.57 \times 10^{-8}$
B $\beta$	6	26252.0	0.1793	114.1	$3.42 \times 10^{-9}$
B $\gamma$	7	21655.0	0.0655	138.3	$1.09 \times 10^{-9}$

(Rubio-Martín, Hernández-Monteagudo & Sunyaev 2005)

# The linear term

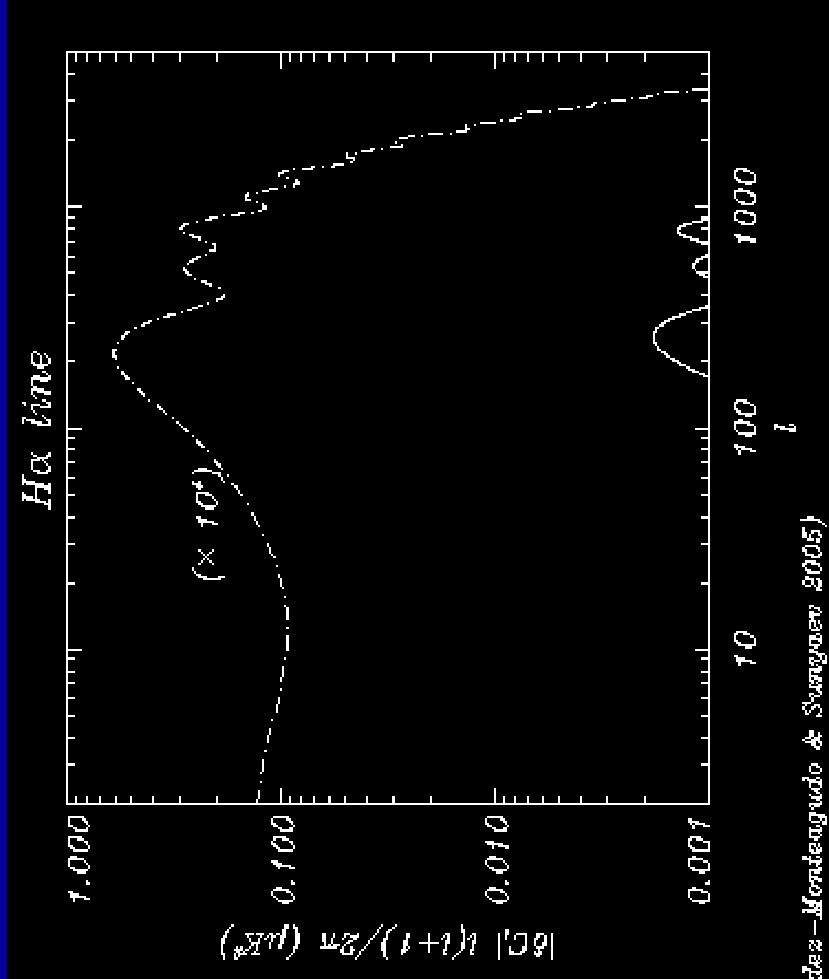
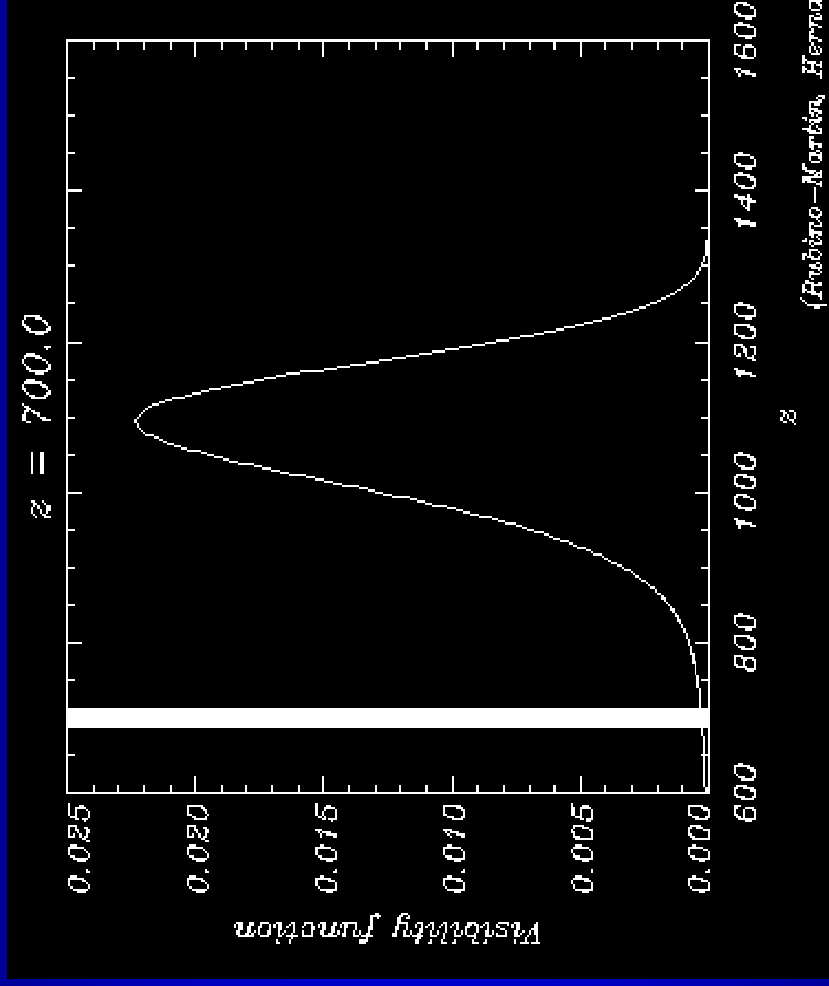


(Rubino-Martin, Hernandez-Montenegro & Sunyaev 2005)

- Optical depths in the lines are very small: this term is sufficient.
- For a given line, this redshift interval translates into frequency interval.

( see additional movies at <http://www.iac.es/galeria/jalberto> )

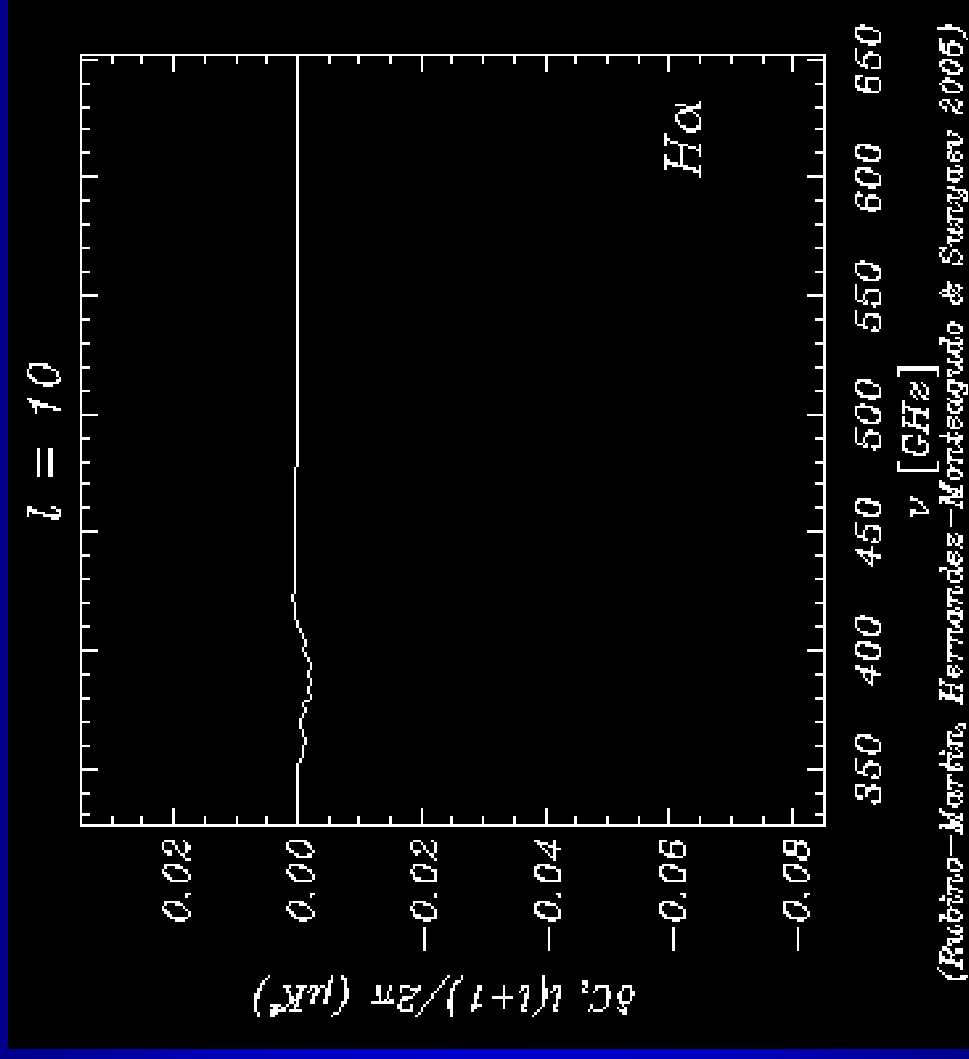
# The H $\alpha$ line



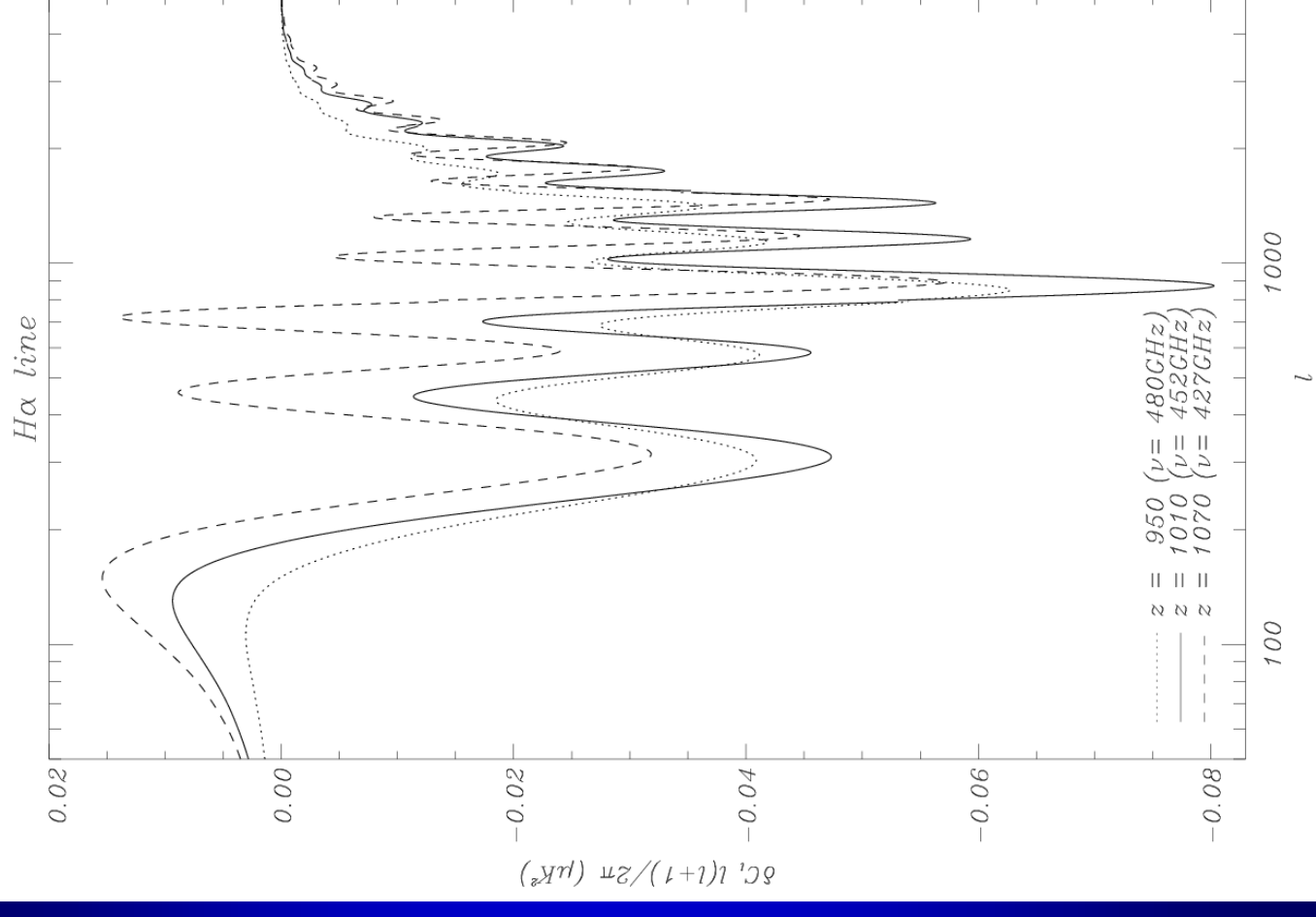
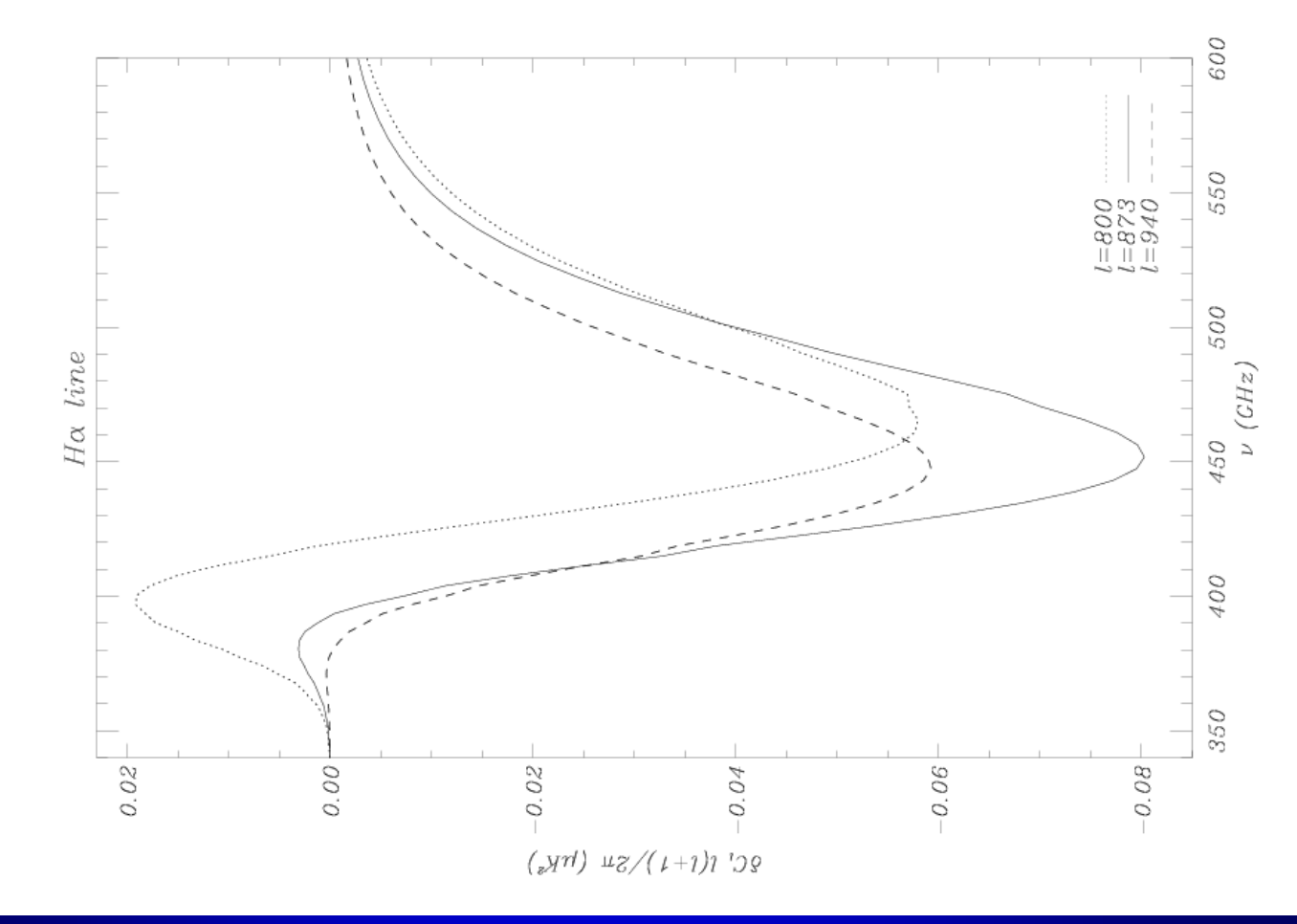
(Rubino-Martín, Hernández-Monteagudo & Sauragen 2005)

The redshift translates into frequency as  $6562.8\text{\AA} (1+z)$

# The H $\alpha$ line (III)



# The H $\alpha$ line (III)

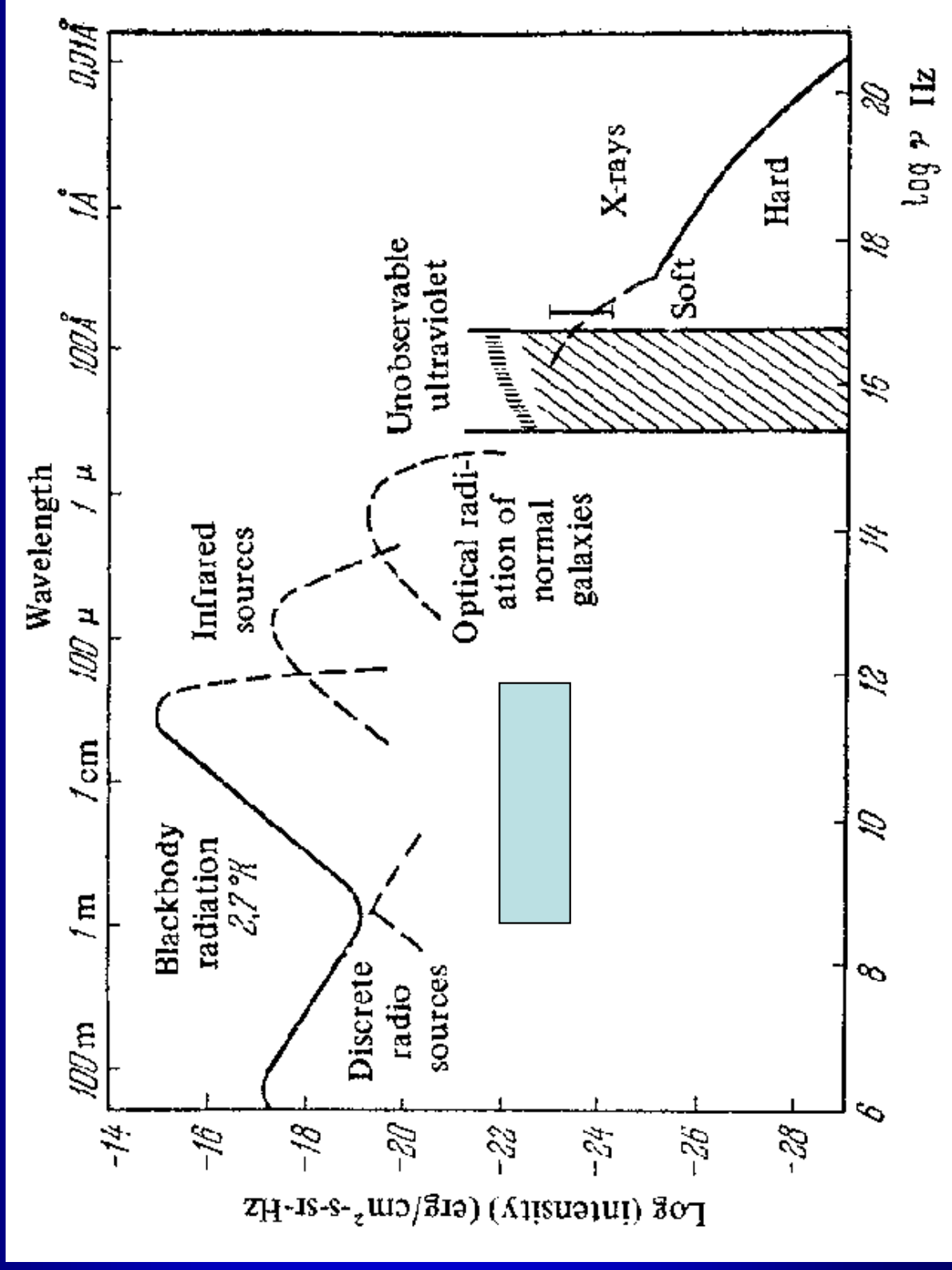


# Observability of the effects

The effects that we are discussing are very small, but:

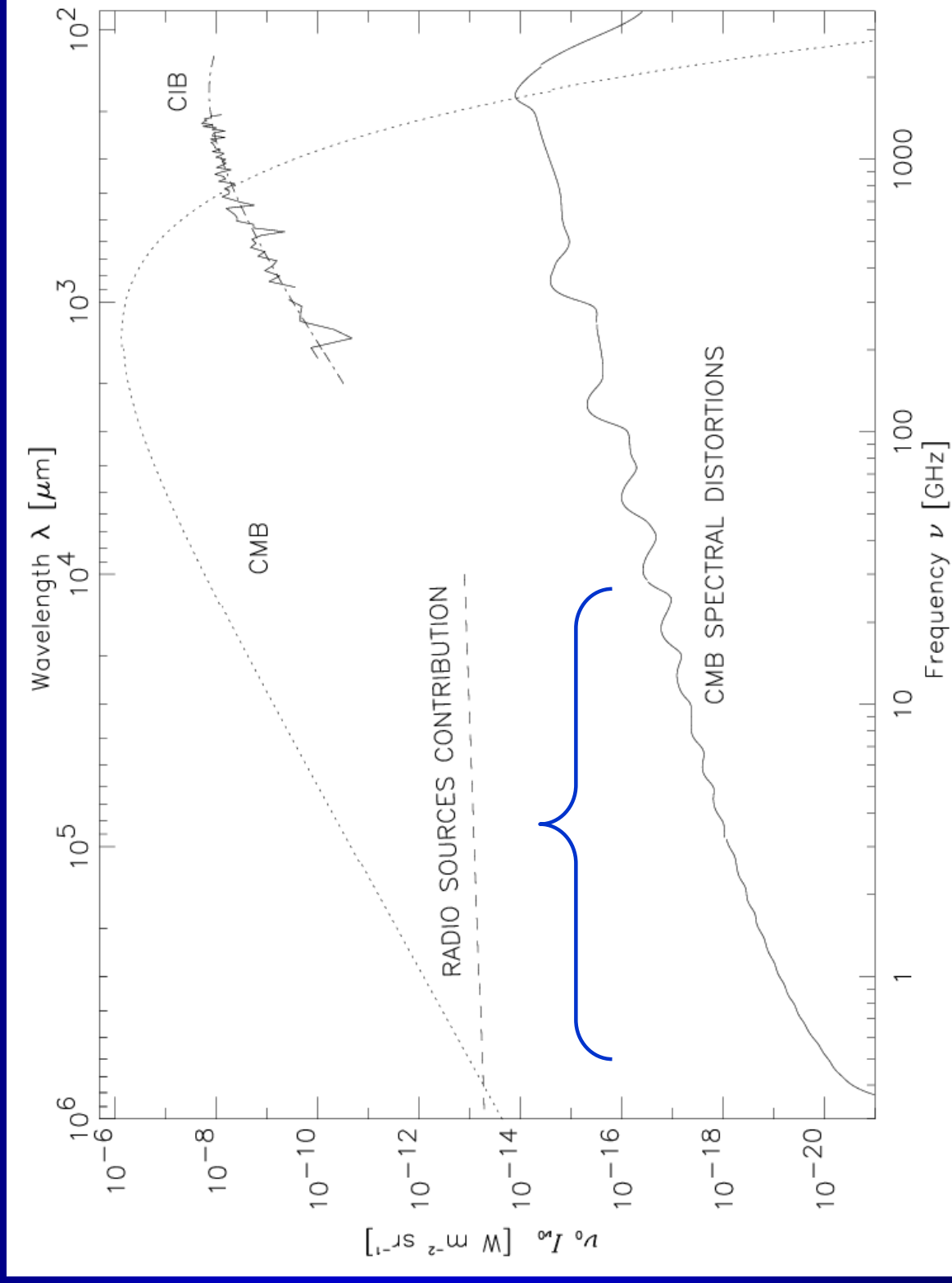
- Fixsen & Mather (2002) point out that current technology permit us to reach the level of  $10^{-7}$  in broad regions of the frequency spectrum.
- Next generation of CMB instruments measuring B-modes (polarization) will reach levels of sub-microkelvin (0.01-0.1  $\mu\text{K}$ ), which is enough to detect these effects on the power spectrum.
- But we will be limited by the control of foregrounds (radiogalaxies, dust emission,...)
- However, **NO FOREGROUND CAN MIMIC** these features.

# Observability of the effects

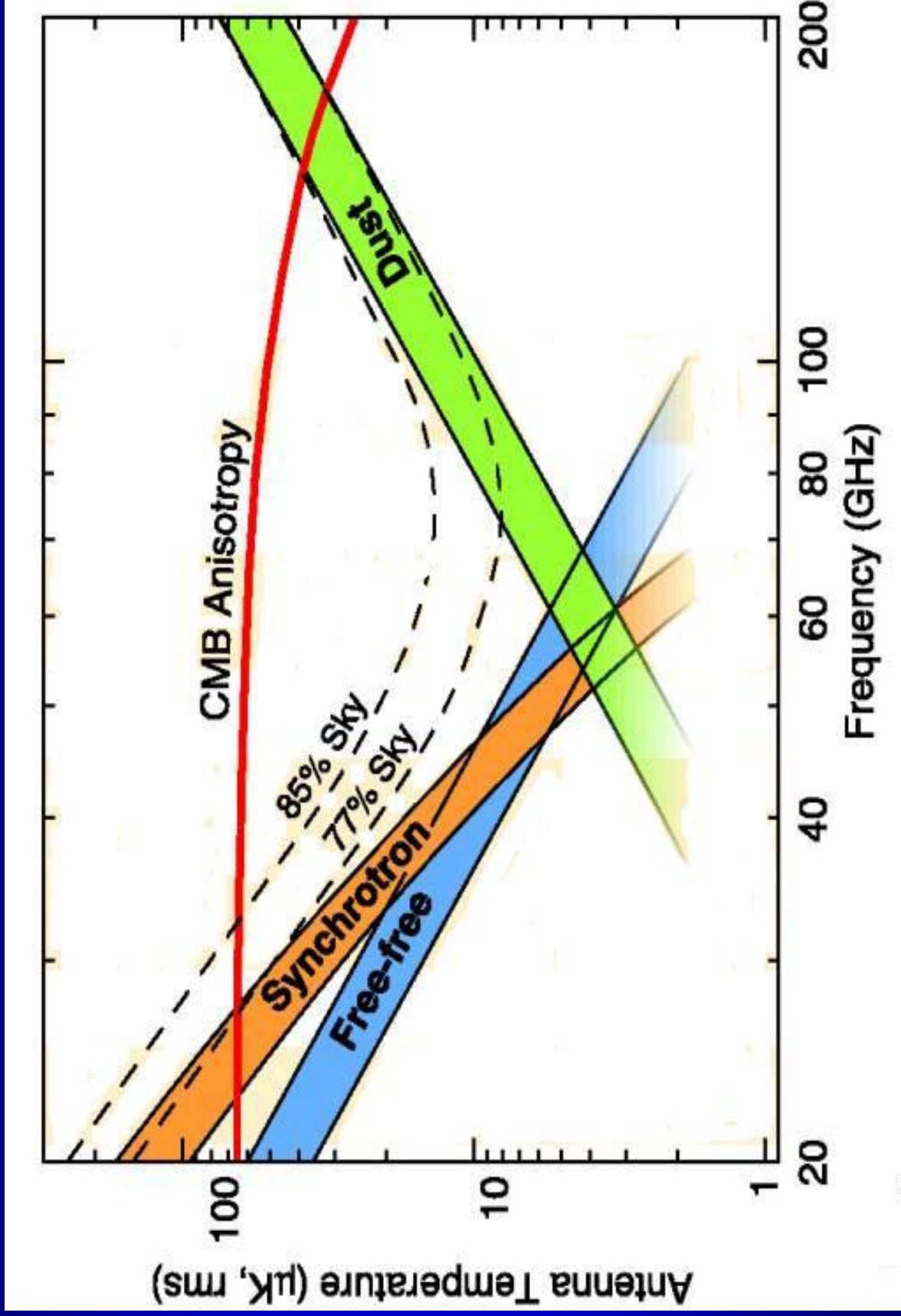


# Observability of the spectral distortions

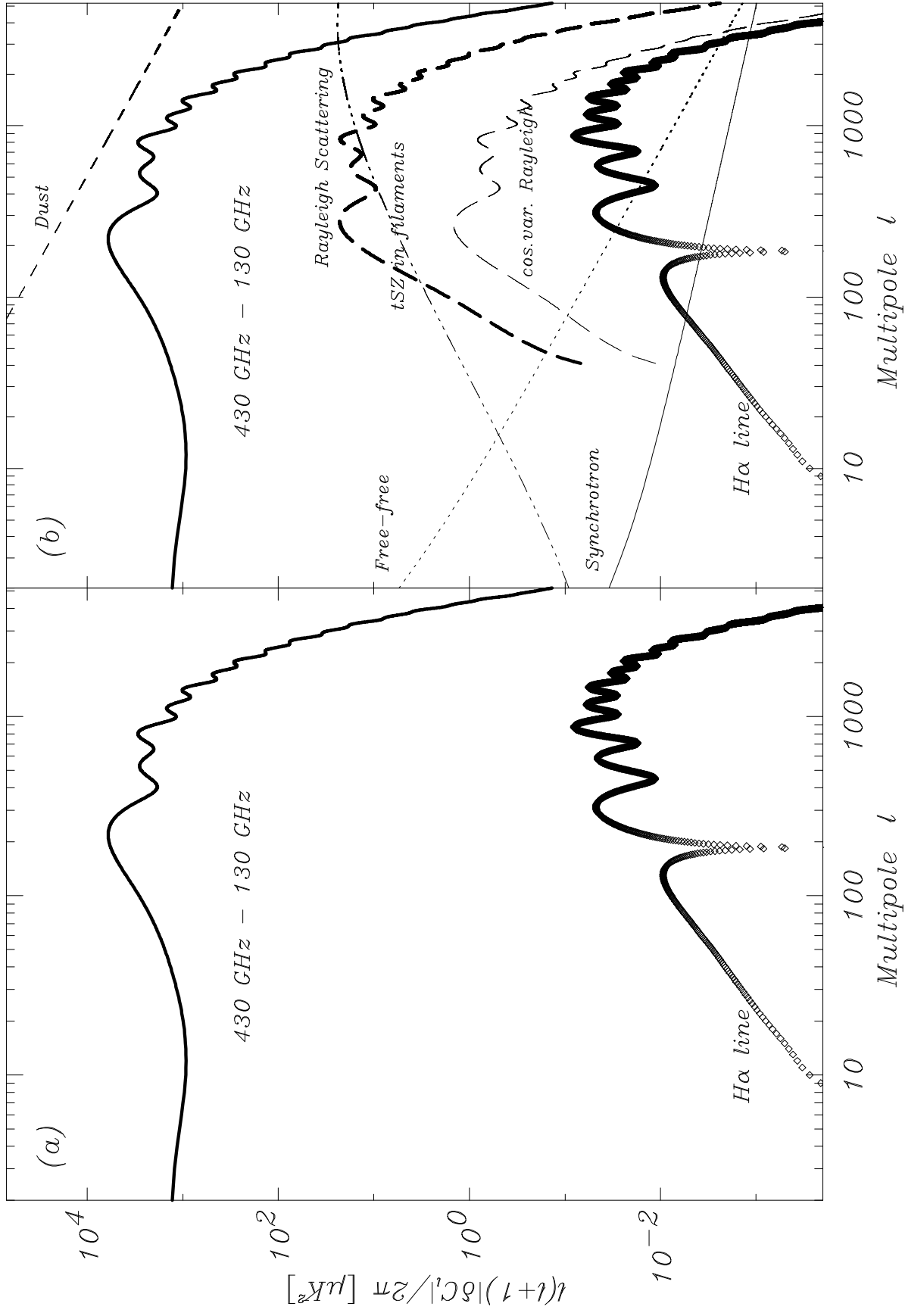
- $\text{Ly}\alpha$  is dominant, but the CIB is intense.
- However, the sensitivity is improving: e.g. Spitzer (Dole et al. 2006) have resolved practically  $\frac{3}{4}$  of the MIB at 160 microns into luminous IR galaxies at  $z \sim 1$ .
- The region around 21cm seems most promising. In addition, there is new physics there (decaying dark matter particles).



# Observability of the effect on the $C_l$ 's



# Observability of the effect on the $C_l$ 's



# Conclusions

- ❑ We have obtained the most precise determination of the Cosmological Recombination spectrum to date.
- ❑ Spectral features from the epoch of Recombination are **very small**, being of the order of sub-microkelvins for power spectrum distortions, and  $10^{-7}$ - $10^{-8}$  for the spectrum itself.
- ❑ Exquisite control on foreground contamination is essential to measure these features, but ...
- ❑ All these features have a very peculiar oscillatory behaviour which can not be mimiced by any other foreground and might help in separating these lines.
- ❑ Observations of these spectral features provide a **direct measurement** of the epoch of recombination, as well as an independent determination of cosmological parameters.